014449-1-T

SURFACE FIELD MEASUREMENTS ON SCALE MODEL F-111 AIRCRAFT

By

Valdis V. Liepa

The Radiation Laboratory

Department of Electrical and Computer Engineering

The University of Michigan

Ann Arbor, Michigan 48109

September 1977

ABSTRACT

Data have been obtained for the current and charge induced on a scale model F-111 aircraft when illuminated by a plane electromagnetic wave in a simulated free space environment. The measurements were made on 1/135 and 1/72 scale models over the frequency range 450 - 4000 MHz, simulating 3.3 - 55.7 MHz full scale. The test points and the types of excitations were chosen to correspond to those used in the full scale measurements in the ARES facility at Kirtland Air Force Base.

PREFACE

It is a pleasure to acknowledge the assistance of Messrs. K. Powers, R. Stoddard, J. Tedesco, and K. Young in performing the measurements, computer programming, data processing, model preparation, and other tasks needed to obtain these data. Special thanks go to Mr. I. LaHaie who spent many frustrating hours in the process of interfacing the HP9830A calculator with the University of Michigan computer. The help provided by the Computing Center personnel, especially Mr. Dave Flower, is also acknowledged.

TABLE OF CONTENTS

Section		Page
	Abstract	i
	Preface	ii
I	INTRODUCTION	1
II	MEASUREMENTS	2
III	DATA	8

TABLE OF ILLUSTRATIONS

Figure No.		Page
1.	1/135 and 1/72 scale models of the F-111 aircraft	4
2.	Charge sensor mounted on the wing of the 1/72 scale model at TP:364	5
3.	Measurement of the current on top of the fuselage at TP:364, shown as oriented in the chamber: top incidence, E-parallel to fuselage	7
4.	Measurement points on F-111. The measurements were made at encircled stations only	9
5.	Directions of measured surface current components	11
6-32.	Data plots	15-41

SECTION I

INTRODUCTION

The data presented here were obtained for the Mission Research Corporation (MRC) to assist in extrapolating [1] the results of full scale tests made in an EMP simulator, and the test points and excitation conditions were chosen to correspond to those used in measurements made in the ARES facility at Kirtland Air Force Base. The data were recorded, reduced and plotted digitally, and have also been furnished to MRC in digital form on computer cards, as well as stored on (IBM compatible) magnetic tape. So as not to lose information that may be relevant to the development of analytical techniques such as SEM, no smoothing has been carried out to remove the minor perturbations attributable to measurement noise, nor have any corrections been applied to account for probe integration. Based on previous measurements performed using clean cylindrical and spherical bodies, probe correction factors have been developed [2] which could be applied to the data in digital form were it found desirable to do so.

---

1. Carl E. Baum, "Extrapolation Techniques for Interpreting the Results of Tests in EMP Simulators in Terms of EMP Criteria", AFWL Sensors & Simulation Notes, Note 222, 1977.
2. Valdis V. Liepa, "Sweep Frequency Surface Field Measurements", University of Michigan Radiation Lab Report No. 013378-1-F, AFWL-TR-75-217, 1975.

SECTION II

MEASUREMENTS

For the most part the measurement techniques are the same as previously used [3], but two changes that were made are the use of a new and larger anechoic chamber [4] and the direct digitization and recording of the data. The measurements were performed over the three bands 450 - 1100, 1000 - 2000 and 2000 - 4000 MHz, using 1/135 and 1/72 scale model F-111 aircraft. There were two models of each scale size, one for current (J) and one for charge (Q) measurements. Based on the actual dimensions of the F-111A, the precise scaling factors for the models are presented in Table 1. These were employed to convert a measurement frequency to a full scale one using the fuselage scale for the case of E-parallel to the fuselage and the wingspan scale for the case of E-perpendicular to the fuselage. The table also gives the measured local (surface) radii of the equivalent cylinders at the test points 181, 150 and 382. These would be needed for adjustment of the data for probe integration effects were it found desirable to incorporate such corrections.

---

3. Valdis V. Liepa, "Surface Field Measurements on Scale Model EC-135 Aircraft", Univ. of Michigan Radiation Lab Report No. 014182-1-F, AFWL-TR-77-101, 1977.
4. Valdis V. Liepa, "Surface Field Measurements on Scale Model E-4 Aircraft", Univ. of Michigan Radiation Lab Report No. 014182-2-F, AFWL-TR-77-111, 1977.

Table 1

Scale Factors for the Models

(Full scale dimensions used (radome removed): length = 19.63 m, wingspan = 19.20 m)

Size	J/Q	Fuselage	Wingspan	Local Surface Curvature Radius At		
				TP:181	TP:150	TP:382
1/72	J	72.03	72.82	0.95 cm	1.43 cm	flat
1/72	Q	71.91	72.77	0.95 cm	1.43 cm	flat
1/135	J	136.79	141.71	0.53 cm	1.27 cm	flat
1/135	Q	137.15	134.4	0.53 cm	1.27 cm	flat

The currents were measured using loops 0.31 cm in outside diameter made from 0.76 mm diameter 50 ohm semi-rigid coax and the charges (or normal electric fields) using a 0.2 cm long monopole made by extending the center conductor of the coax. The measurement procedure was to make all the current measurements on the 1/72 and 1/135 models in one frequency band and then repeat the measurements in each of the other two bands. The process was then repeated for the charge measurements.

Figure 1 is a photograph of the models. The unmodified (smooth) ones on the left were used for the current measurements and the ones on the right for the charge measurements. The patches are adhesive copper tape covering slots cut in the models to accommodate the charge sensors. Figure 2 shows a close-up of the charge sensor mounted on the wing of the 1/72 model at station TP:364. The signal lead passes through the wing and then along the bottom

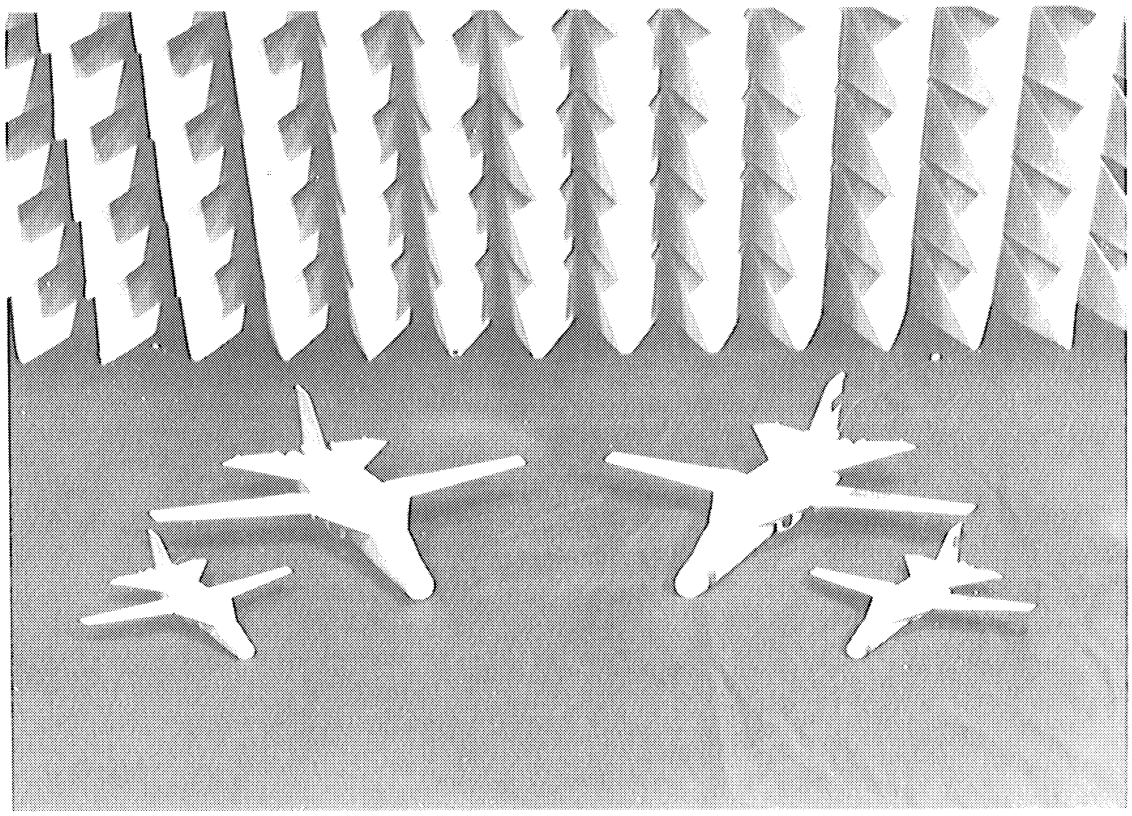

Figure 1: 1/135 and 1/72 scale models of the F-111 aircraft. Those on the left were used for current measurements and those on the right, with patches of copper tape attached, were used for charge measurements.

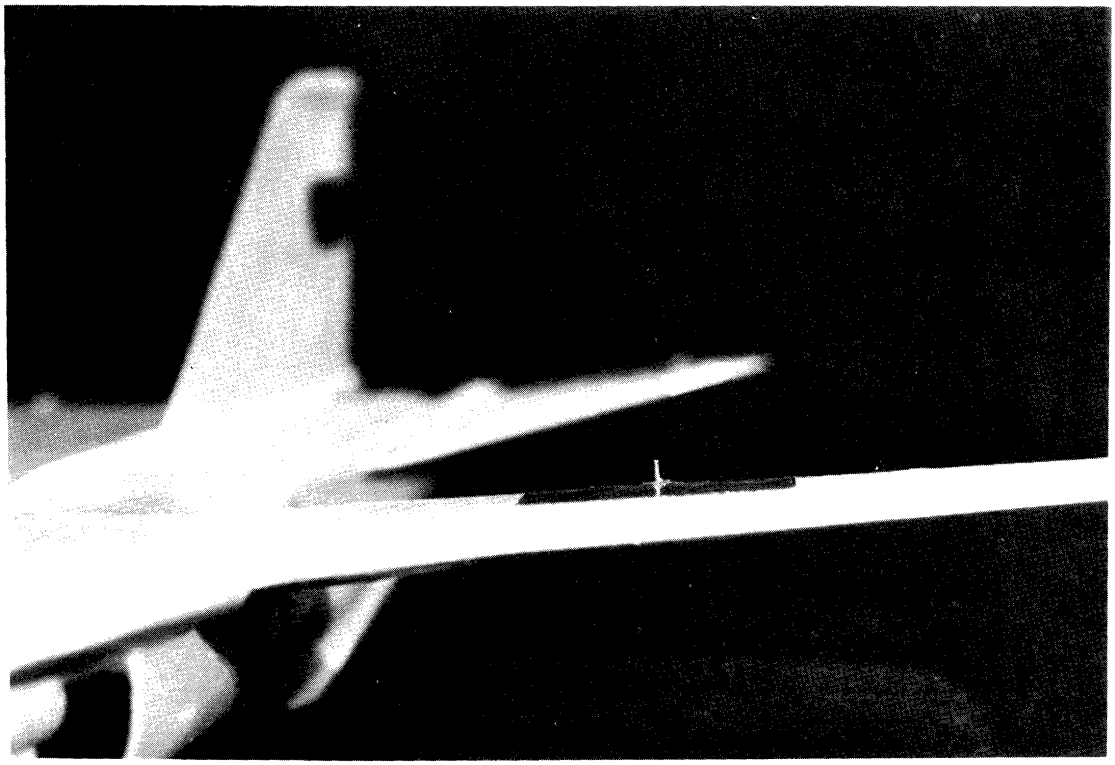

Figure 2: Charge sensor mounted on the wing of the 1/72 scale model at TP:364.

of the fuselage, leaving the model near the trailing edge of the wings. Underneath the wing and on the fuselage the coax is taped to avoid introducing new current paths that could perturb the measurements. The set-up in measuring the current at TP:150 is shown in Figure 3. For this measurement the incidence was topside with electric vector parallel to the fuselage. Note that the sensor lead is perpendicular to the incident electric vector to minimize interaction.

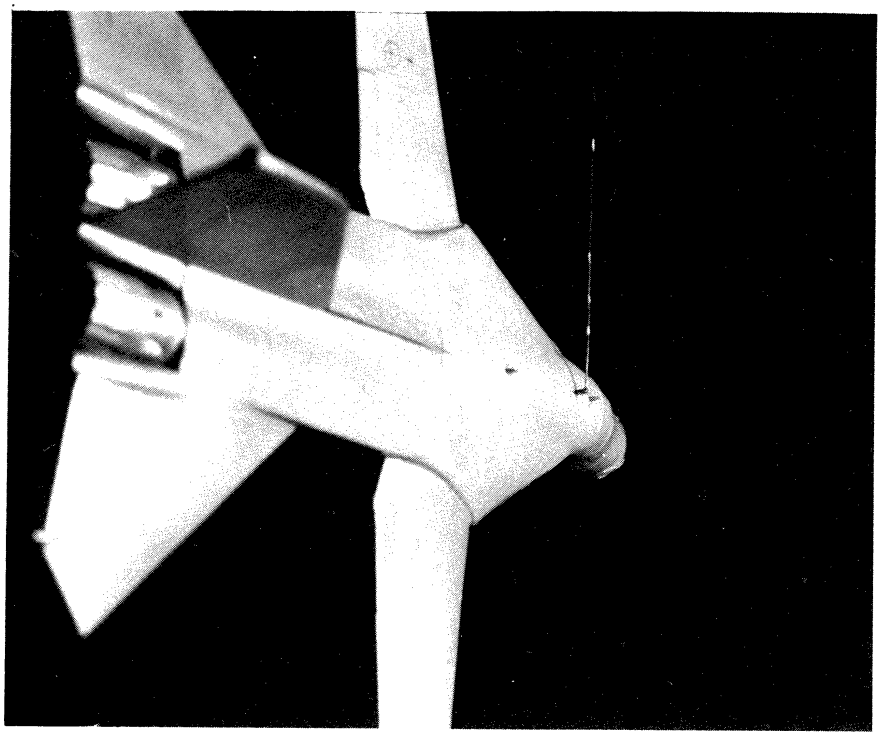

Figure 3: Measurement of the current on top of the fuselage at TP:364, shown as oriented in the chamber: top incidence, E-parallel to fuselage.

SECTION III

DATA

Results are presented for 21 current and 5 charge measurements and the cases considered are summarized in Table 2, p. 14, which can also serve as a guide in finding a particular data set. The locations of the test points are shown in Figure 4, but the corresponding station numbers will also be used to describe these points. In the identification of the station numbers the letter abbreviations are as follows:

F	-	fuselage
WL	-	water line
LBL	-	left buttock line
T	-	top of the aircraft
B	-	bottom of the aircraft

The number between the letters is the distance in inches on the full scale aircraft. For the distances measured along the fuselage (radome removed), the numbers start from 114.25 at the front and increase to 887.107 at the rear-most point which is at the top of the vertical stabilizer. For the wing stations two numbers are used, one giving the distance from the front of the aircraft and the other the distance out from the plane of symmetry.

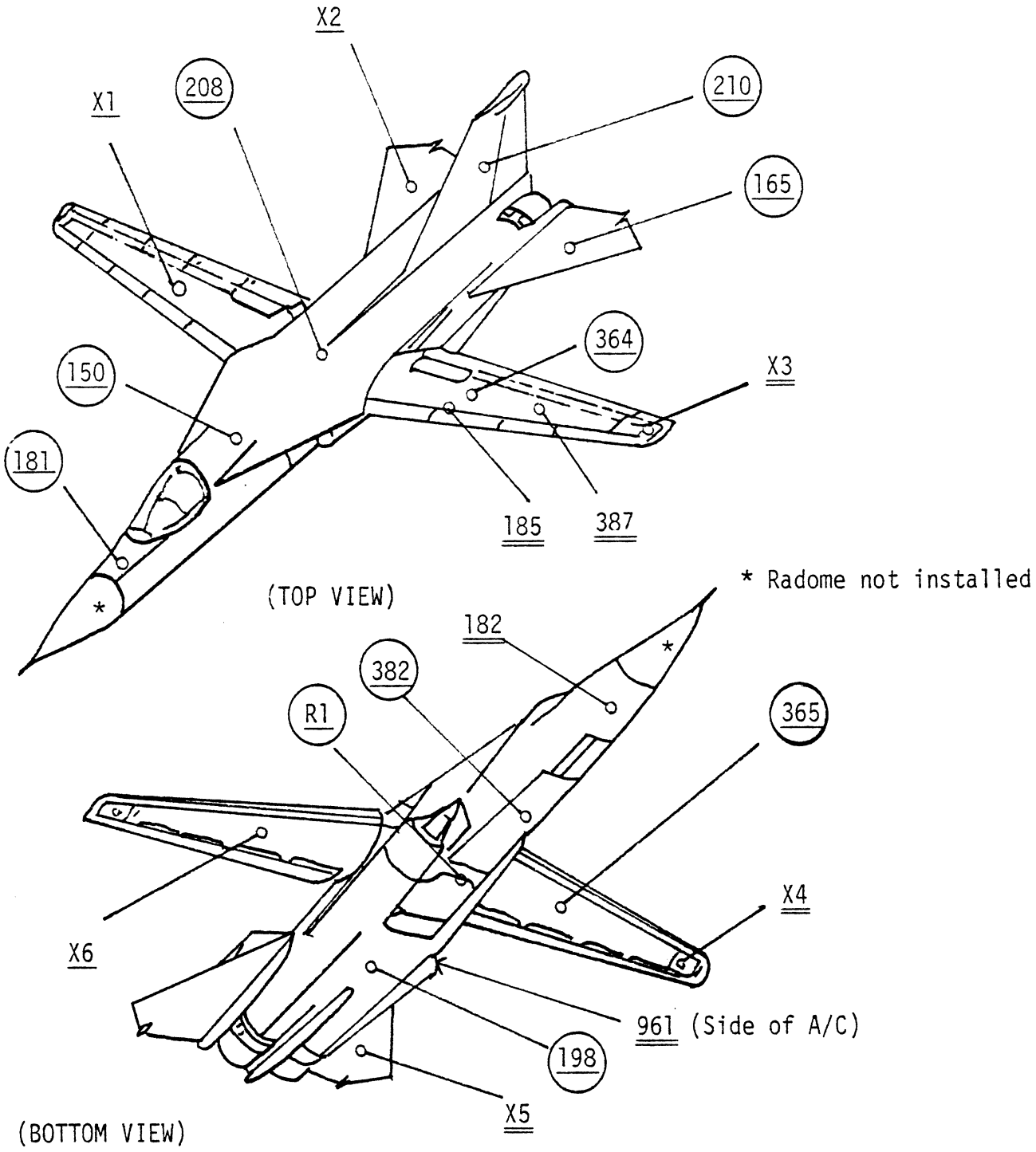

Figure 4: Measurement points on F-111. The measurements were made at encircled stations only.

The particular measurement situation is described in the information contained on each figure. As an example, consider Figure 7. The title at the top gives the test point location (TP:181), the polarization (PAR, i.e. electric field parallel to the fuselage), the quantity measured (Q), and the file names where the data is stored (F603, ..., F528). As a further aid, a sketch is included showing the measurement point, the direction of incidence, and the polarization.

The current and charge data are normalized to the incident fields H_o and E_o, respectively, measured at TP:150 (F352T) without the model present. TP:150 is thus the reference origin for the phase. The $e^{i\omega t}$ time convention is used, implying a decrease in phase on moving away from the source. Figure 5 shows the components of the skin currents measured at the various test locations. The word "axial" (J_A) and "circumferential" (J_C) used in describing these components are somewhat arbitrary. Thus, on the wings and horizontal and vertical stabilizers, the components J_A and J_C are actually perpendicular and parallel to the fuselage, respectively. At some of the stations considered, the measured field component would be zero under ideal conditions, and these cases are identified by an asterisk in Table 2 and on the corresponding figures. Since the data have been obtained under practical conditions using actual models in an anechoic chamber, small but non-zero fields are measured even for these cases. Their amplitudes are indicative of the noise or background level and could conceivably be used in an error analysis.

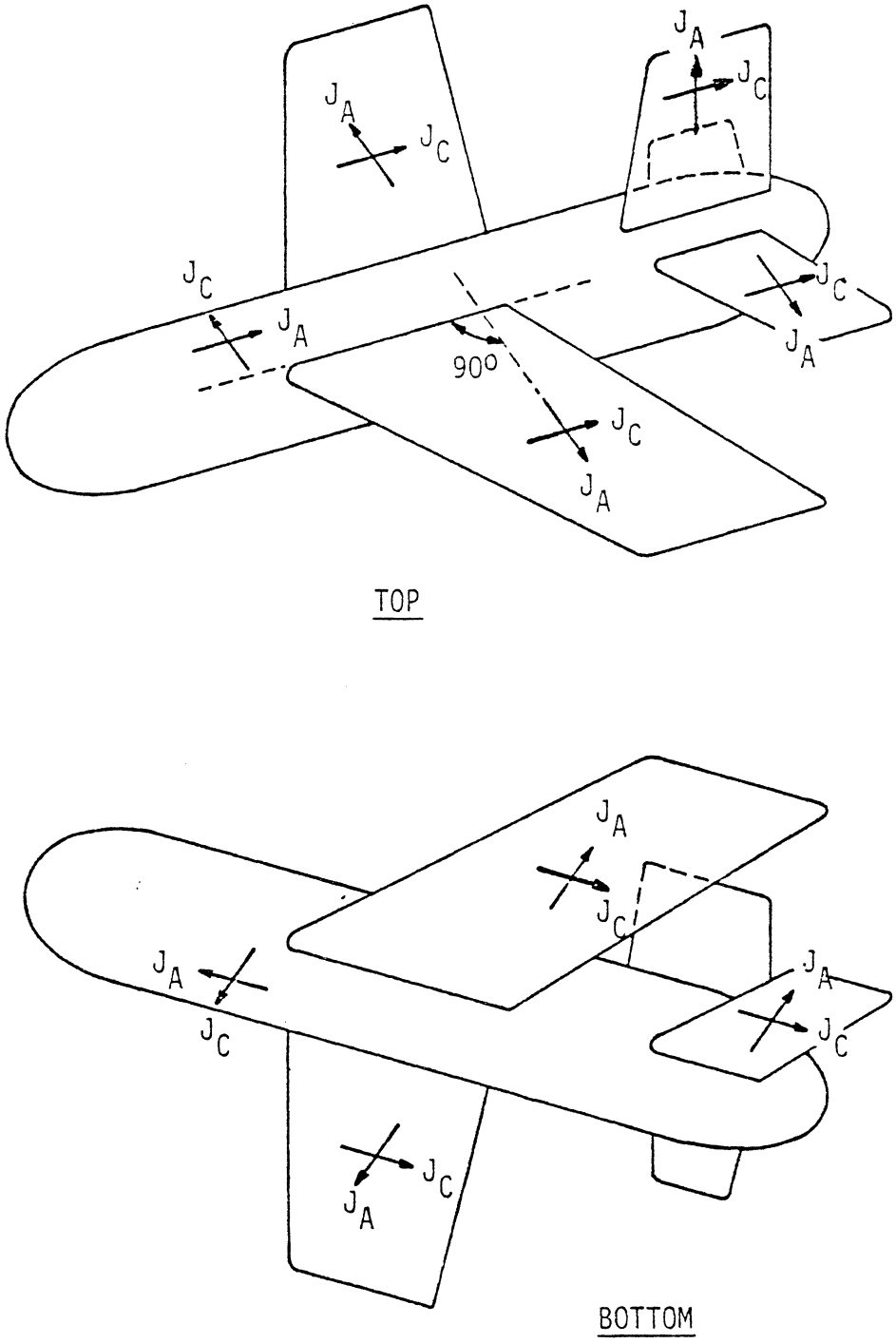

Figure 5: Directions of Measured Surface Current Components.

For those who may require the data in digital form, an illustrative data set is given in Table 3 showing the data used to generate a part of Figure Six data files recorded over three frequency bands with two different scale models are needed to generate the curves in any given case. The data are stored on magnetic tape and can be provided on tape or punched cards to any authorized user. The file format is as follows:

1. FILENAME (4A4)
2. Comments (18A4)
3. Comments (18A4)
4. TITLE used in plotting (18A4)
5. FMIN, FMAX, AMPMIN, AMPMAX, PHASEMIN, PHASEMAX, NN (4F8.3, 2F8.2, I5)
6. F(1) AMP(1) PHASE(1) F(2) AMP(2) PHASE(2) F(3) AMP(3) PHASE(3) (3(2F8.3, F8.2)

data ↕ .... F(NN) AMP(NN) PHASE(NN)

where NN is the number of data points in the set.

Table 3

Illustration of data set.

```
F423
F111/135,150,PAR,JA,1,A,5/20/77

F-111 TP:150 PAR JA;F423,435,459,447,8,1
   3.291   8.101   2.308   6.399  -16.69   48.39  138
   3.291   2.308   43.91   3.326   2.328   44.57   3.361   2.381   44.73
   3.396   2.395   44.37   3.432   2.432   45.10   3.467   2.486   46.42
   3.502   2.529   46.13   3.537   2.572   46.63   3.572   2.621   46.92
   3.607   2.677   46.10   3.642   2.696   46.67   3.677   2.727   47.14
   3.712   2.822   47.50   3.748   2.854   48.05   3.783   2.905   48.39
   3.818   3.018   48.13   3.853   3.056   47.16   3.888   3.095   46.58
   3.923   3.154   46.80   3.958   3.192   46.22   3.993   3.238   45.64
   4.028   3.200   46.25   4.064   3.244   46.86   4.099   3.333   46.77
   4.134   3.368   46.87   4.169   3.452   46.78   4.204   3.535   46.08
   4.239   3.538   45.39   4.274   3.589   45.10   4.309   3.657   45.10
   4.344   3.657   44.72   4.379   3.716   44.83   4.415   3.774   45.15
   4.450   3.842   44.57   4.485   3.928   44.09   4.520   3.978   43.92
   4.555   4.018   43.36   4.590   4.106   43.30   4.625   4.127   42.84
   4.660   4.166   42.69   4.695   4.273   43.05   4.731   4.353   42.12
   4.766   4.422   41.69   4.801   4.533   41.58   4.836   4.594   40.17
   4.871   4.622   39.17   4.906   4.649   39.17   4.941   4.666   38.29
   4.976   4.714   38.52   5.011   4.772   38.56   5.046   4.875   37.70
   5.082   4.935   37.86   5.117   5.007   37.32   5.152   5.113   36.31
   5.187   5.162   36.19   5.222   5.247   35.60   5.257   5.382   34.51
   5.292   5.395   33.63   5.327   5.444   32.77   5.362   5.532   32.32
   5.398   5.556   31.57   5.433   5.619   30.75   5.468   5.709   30.43
   5.503   5.786   29.12   5.538   5.865   27.83   5.573   5.903   27.05
   5.608   5.901   25.78   5.643   5.939   25.02   5.678   5.895   24.48
   5.714   5.962   23.84   5.749   6.085   23.62   5.784   6.139   22.31
   5.819   6.223   21.02   5.854   6.264   20.02   5.889   6.234   18.35
   5.924   6.248   17.49   5.959   6.262   17.24   5.994   6.276   16.09
   6.029   6.350   15.17   6.065   6.351   14.14   6.100   6.382   12.74
   6.135   6.399   11.94   6.170   6.344   10.55   6.205   6.348    9.27
   6.240   6.324    9.00   6.275   6.286    7.74   6.310   6.279    6.88
   6.345   6.214    6.24   6.381   6.180    5.20   6.416   6.203    4.77
   6.451   6.171    3.95   6.486   6.197    3.03   6.521   6.195    2.72
   6.556   6.152    1.61   6.591   6.181    0.61   6.626   6.169   -0.39
   6.661   6.087   -2.08   6.696   6.008   -3.17   6.732   5.876   -3.66
   6.767   5.788   -4.15   6.802   5.742   -4.03   6.837   5.711   -4.31
   6.872   5.733   -5.00   6.907   5.719   -5.18   6.942   5.703   -6.36
   6.977   5.703   -7.35   7.012   5.612   -8.03   7.048   5.562   -8.62
   7.083   5.514   -9.21   7.118   5.442   -9.71   7.153   5.422  -10.31
   7.188   5.390  -10.91   7.223   5.322  -11.62   7.258   5.268  -12.13
   7.293   5.180  -12.45   7.328   5.106  -12.57   7.364   5.091  -12.50
   7.399   5.043  -12.54   7.434   5.019  -12.98   7.469   5.018  -13.03
   7.504   4.972  -13.69   7.539   4.927  -14.15   7.574   4.917  -14.13
   7.609   4.873  -14.81   7.644   4.819  -15.01   7.679   4.783  -15.40
   7.715   4.747  -15.81   7.750   4.684  -16.33   7.785   4.591  -16.46
   7.820   4.521  -16.69   7.855   4.452  -16.24   7.890   4.404  -15.88
   7.925   4.357  -15.55   7.960   4.350  -15.02   7.995   4.354  -14.90
   8.031   4.337  -15.19   8.066   4.310  -15.28   8.101   4.254  -15.49
```

Table 2

Summary of Measurements

Test Point	Station Number	E ∥ Fuselage			E ⊥ Fuselage		
		J_A	J_C	Q	J_A	J_C	Q
181	F160T			Fig. 6			
150	F352T	Fig. 7				Fig. 8	
382	F337.5B	9				10	
208	F520T	11	Fig. 12*		Fig. 13*	14	
R1	F469B	15	16*		17*	18	
198	F640B	19				20	
210	F825T WL265	21	22	23			
165	F830T LBL130	24	25	26	27	28	
364	F550T LBL180				29		Fig. 30
365	F550B LBL180				31		32

* null field measurements; see page 10.

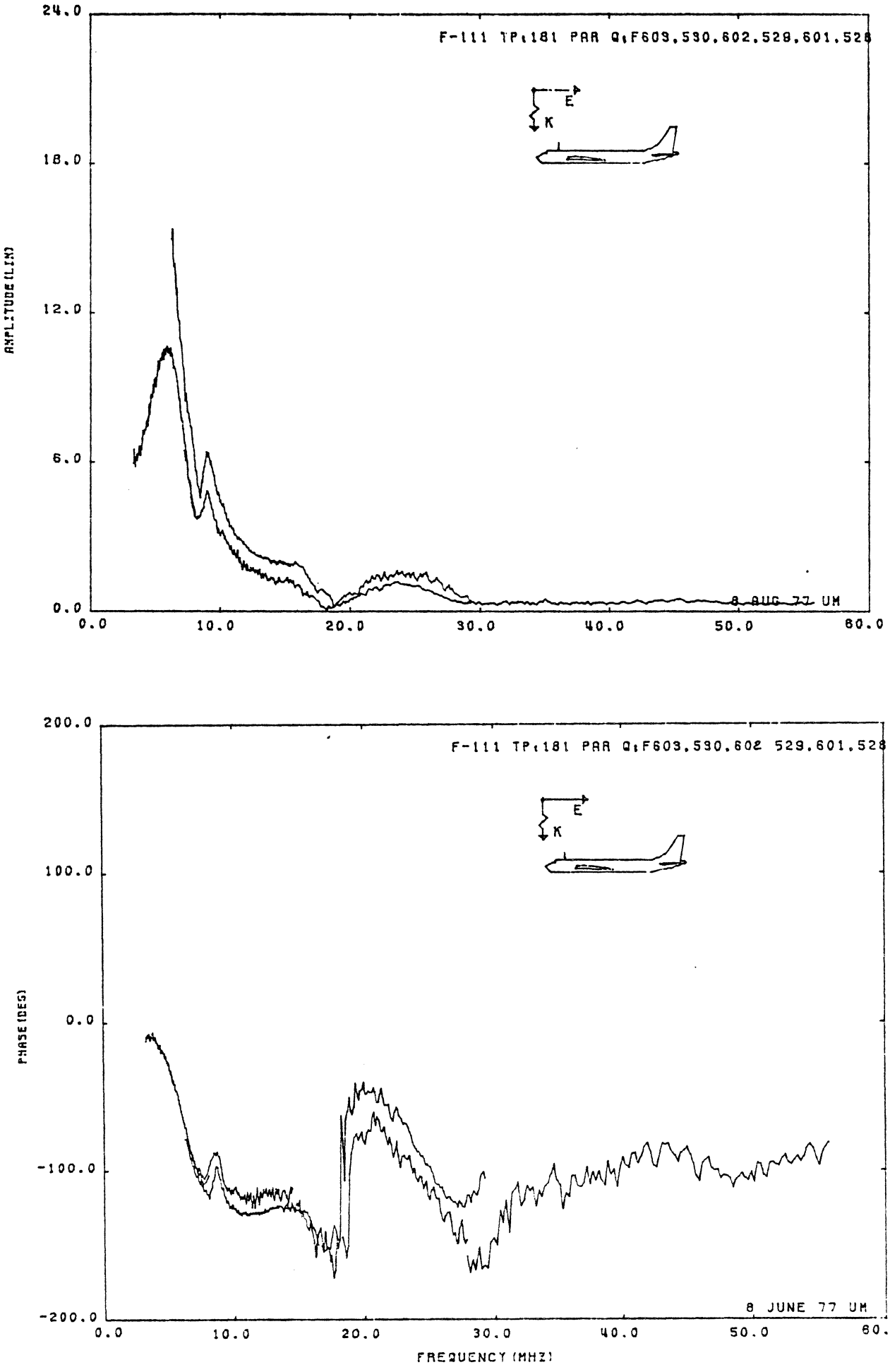

Figure 6: Charge at TP:181, E-parallel to fuselage.

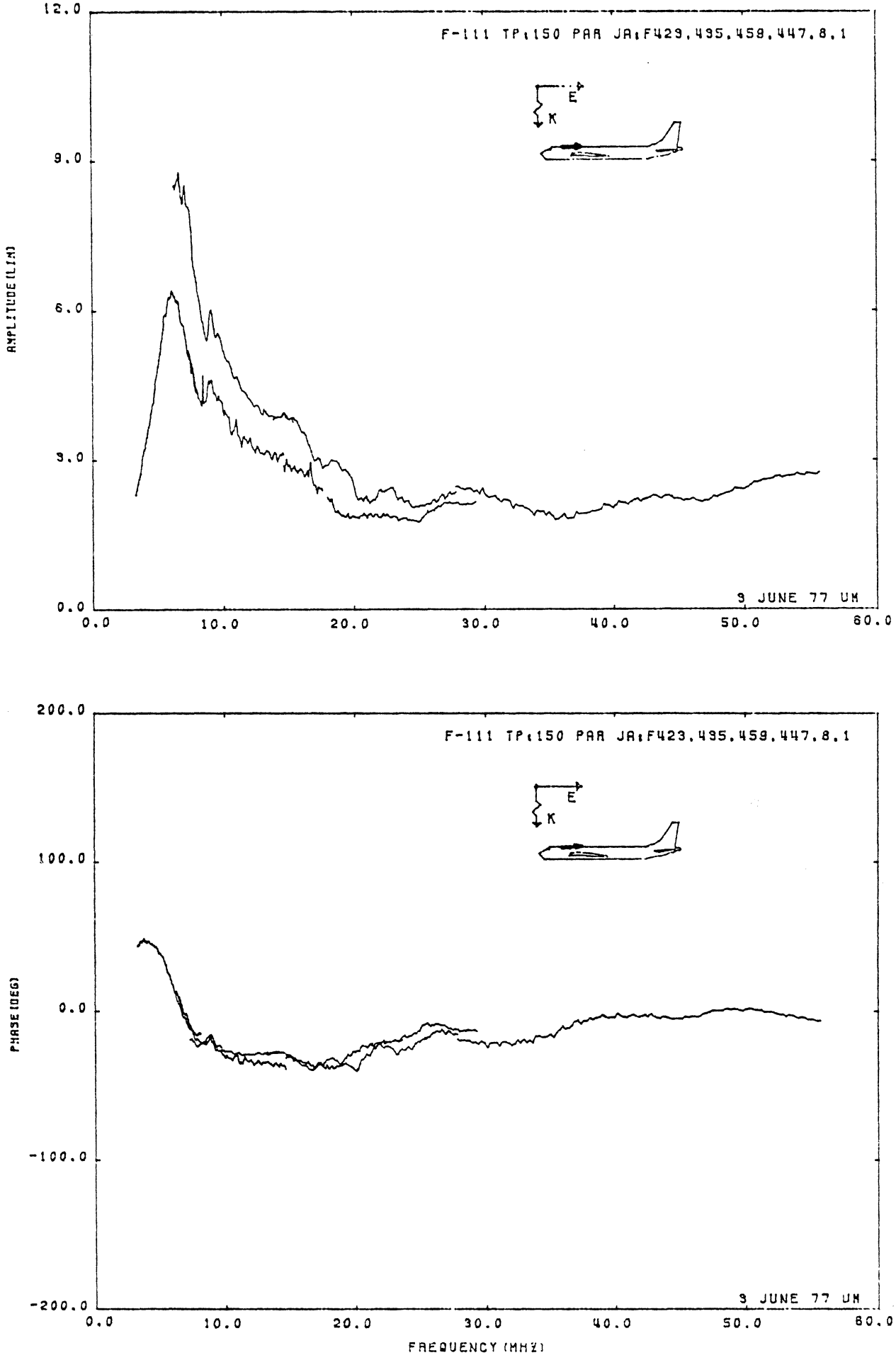

Figure 7: Axial current at TP:150, E-parallel to fuselage.

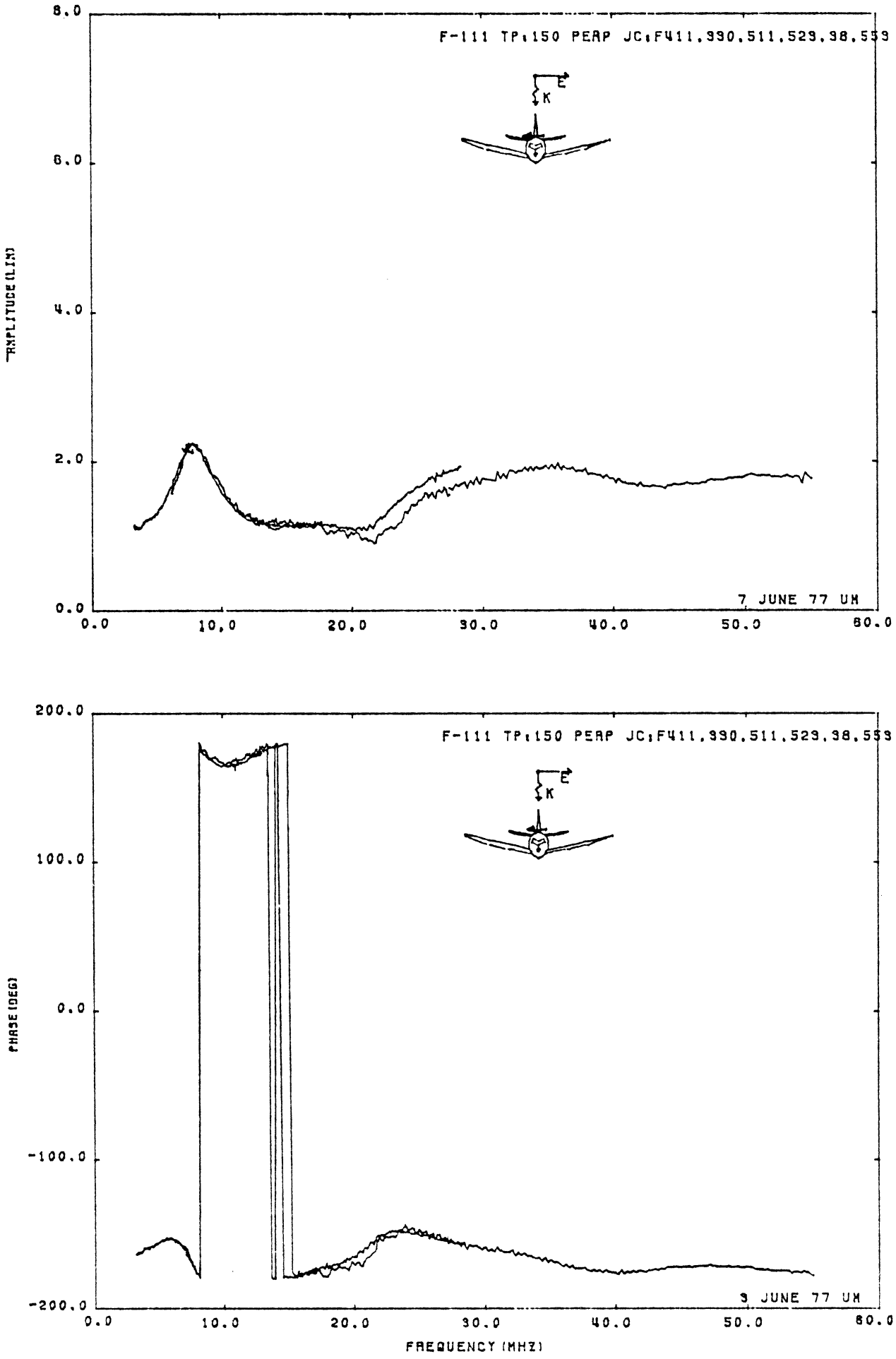

Figure 8: Circumferential current at TP:150, E-perpendicular to fuselage.

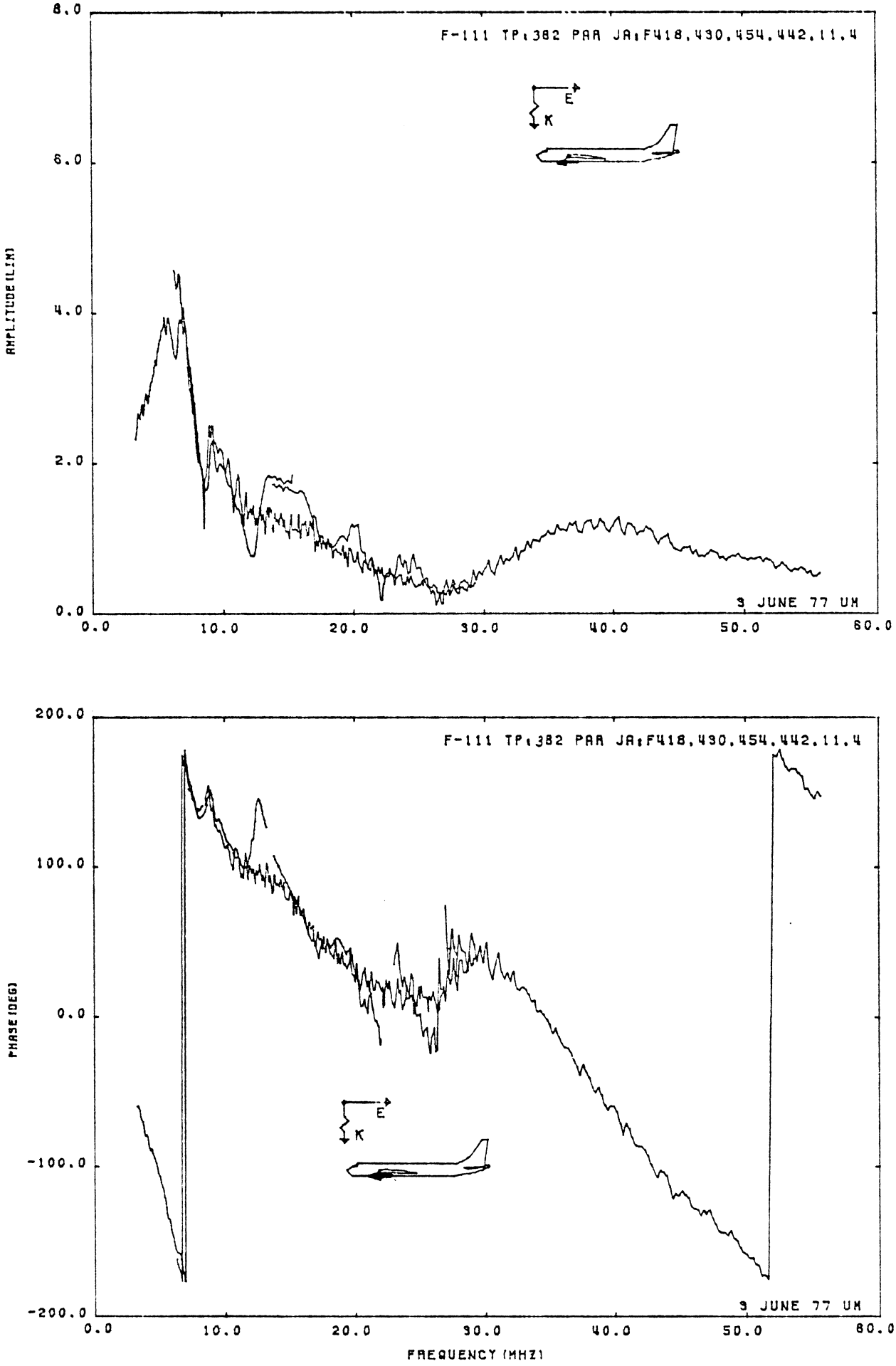

Figure 9: Axial current at TP:382, E-parallel to fuselage.

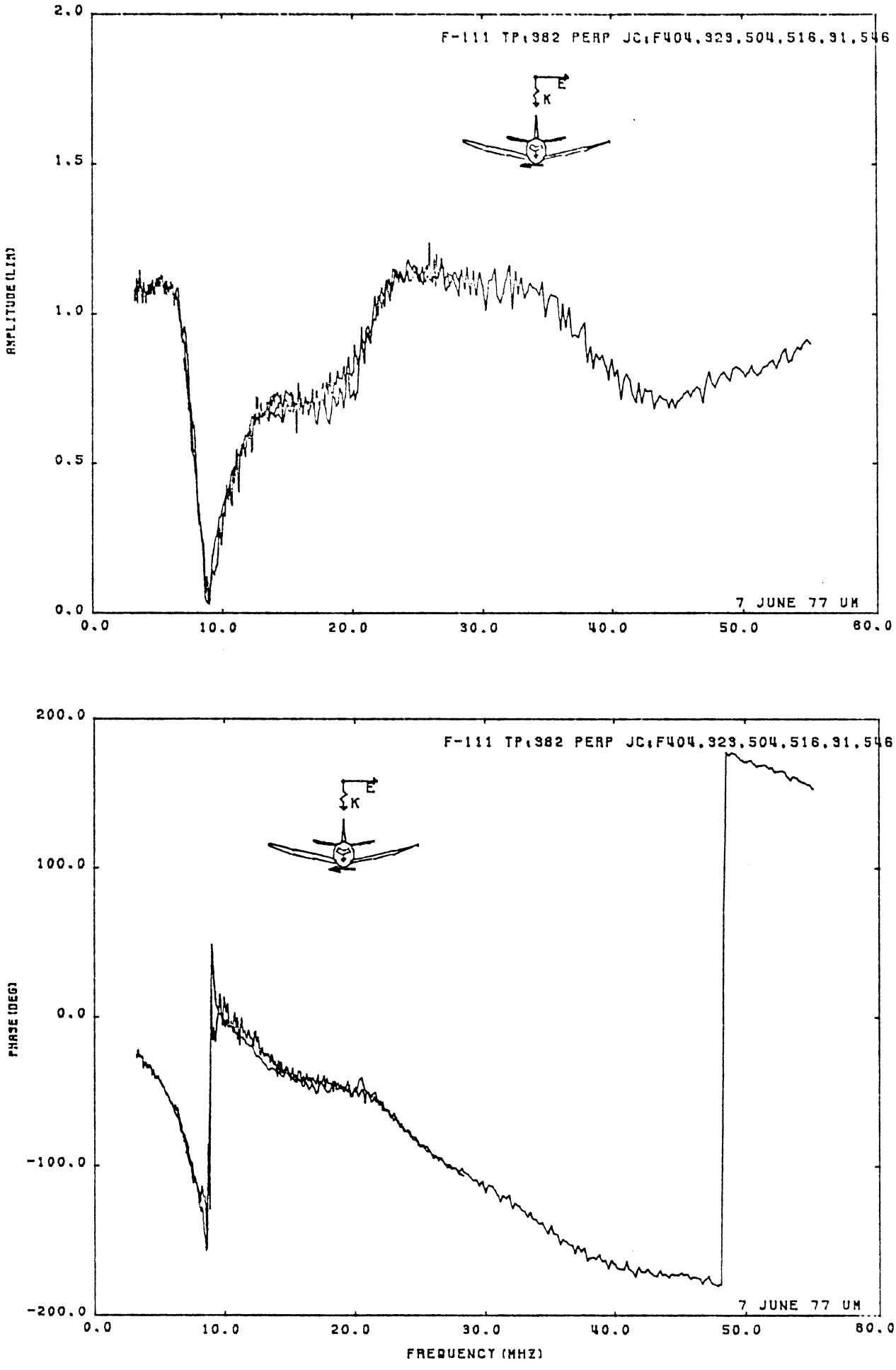

Figure 10: Circumferential current at TP:382, E-perpendicular to fuselage.

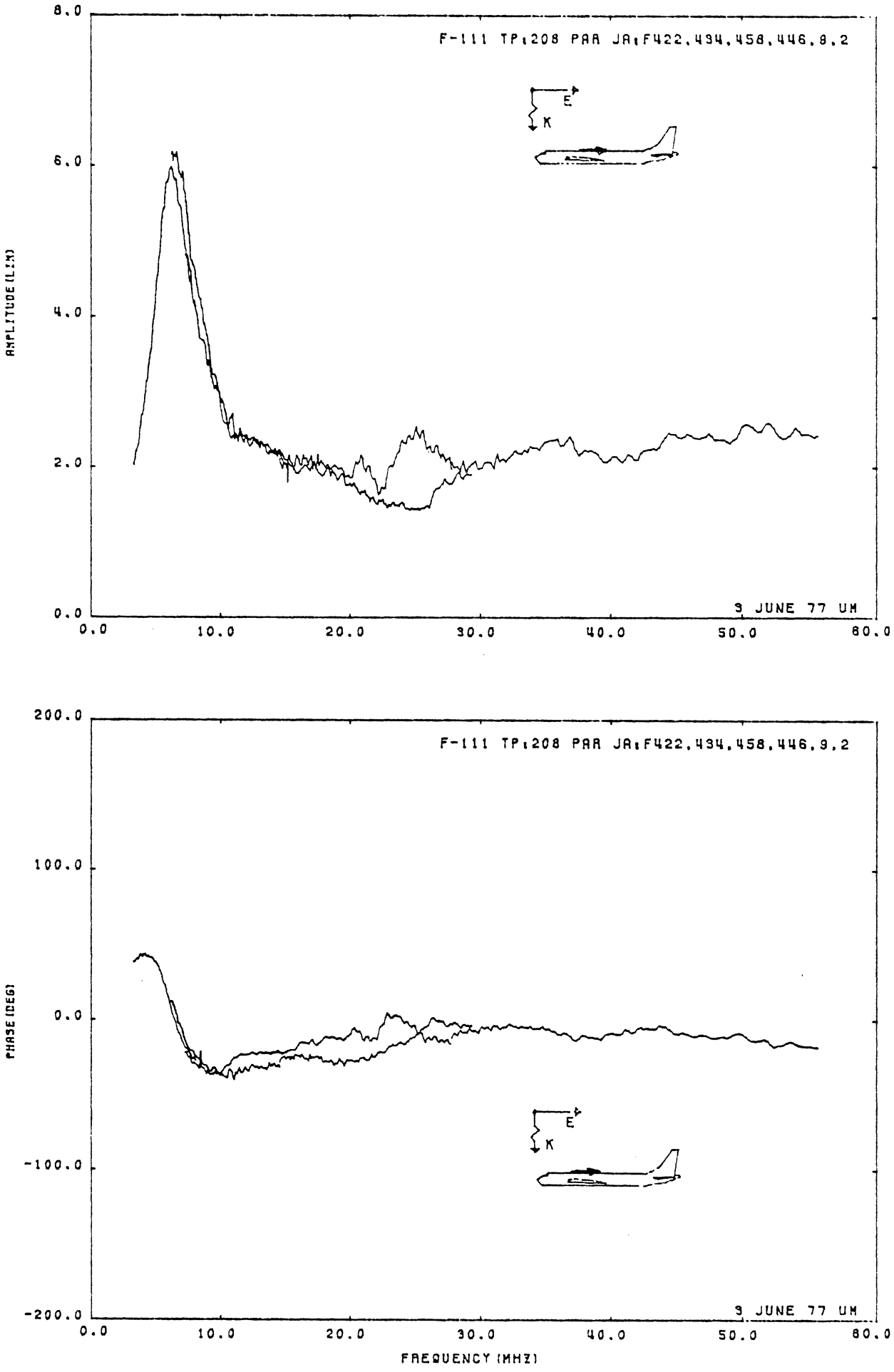

Figure 11: Axial current at TP:208, E-parallel to fuselage.

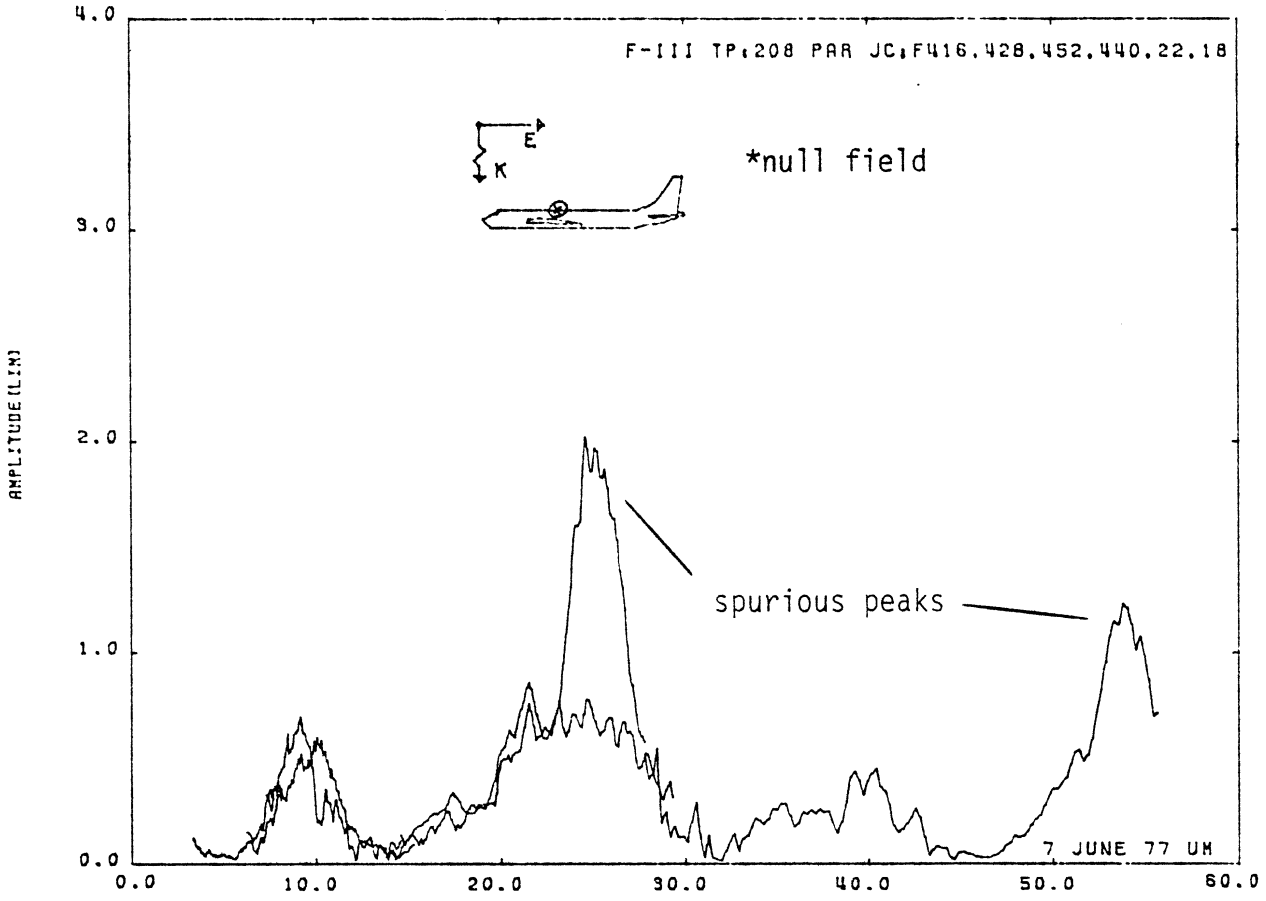

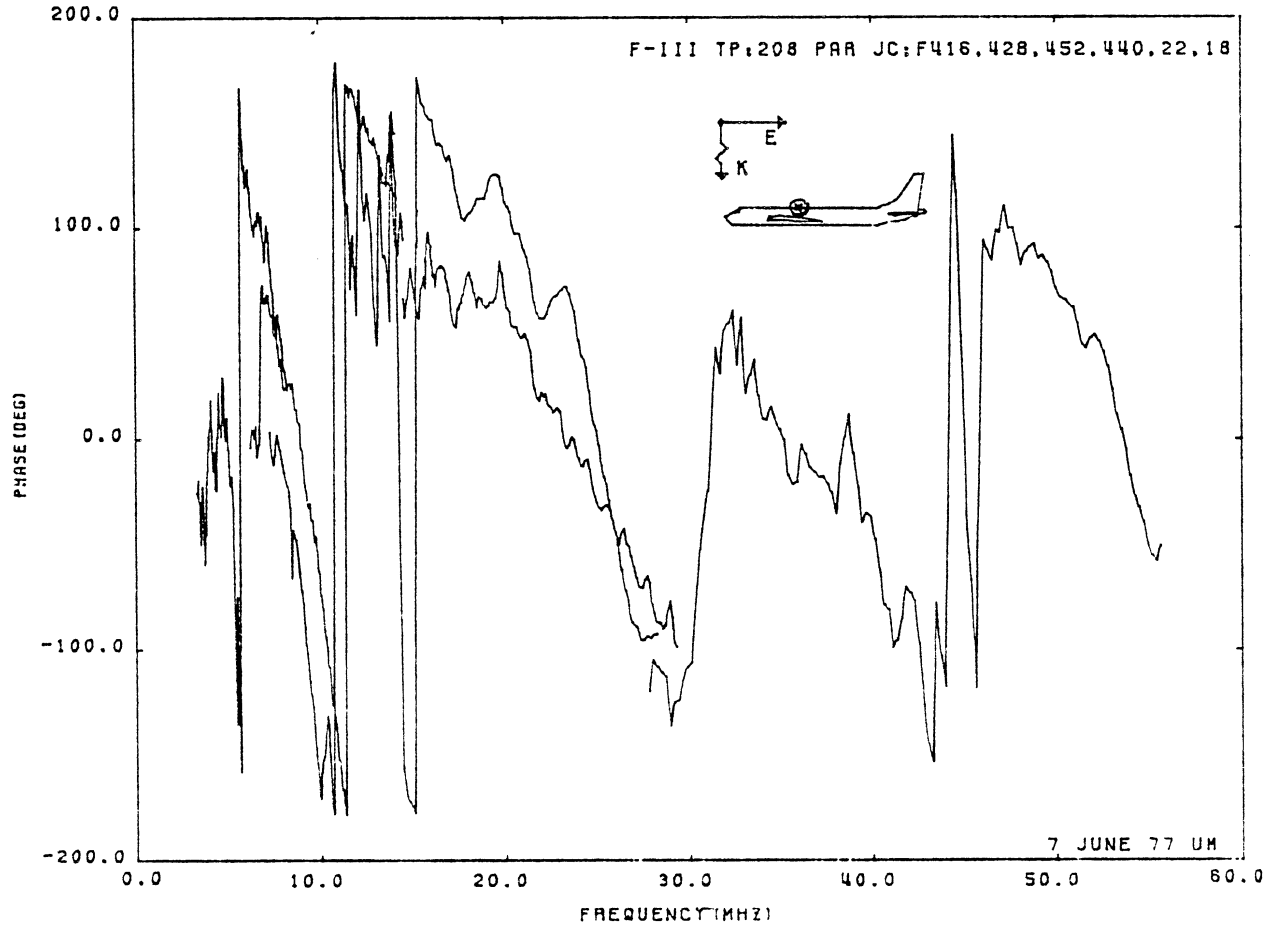

Figure 12: Circumferential current at TP:208, E-parallel to fuselage.

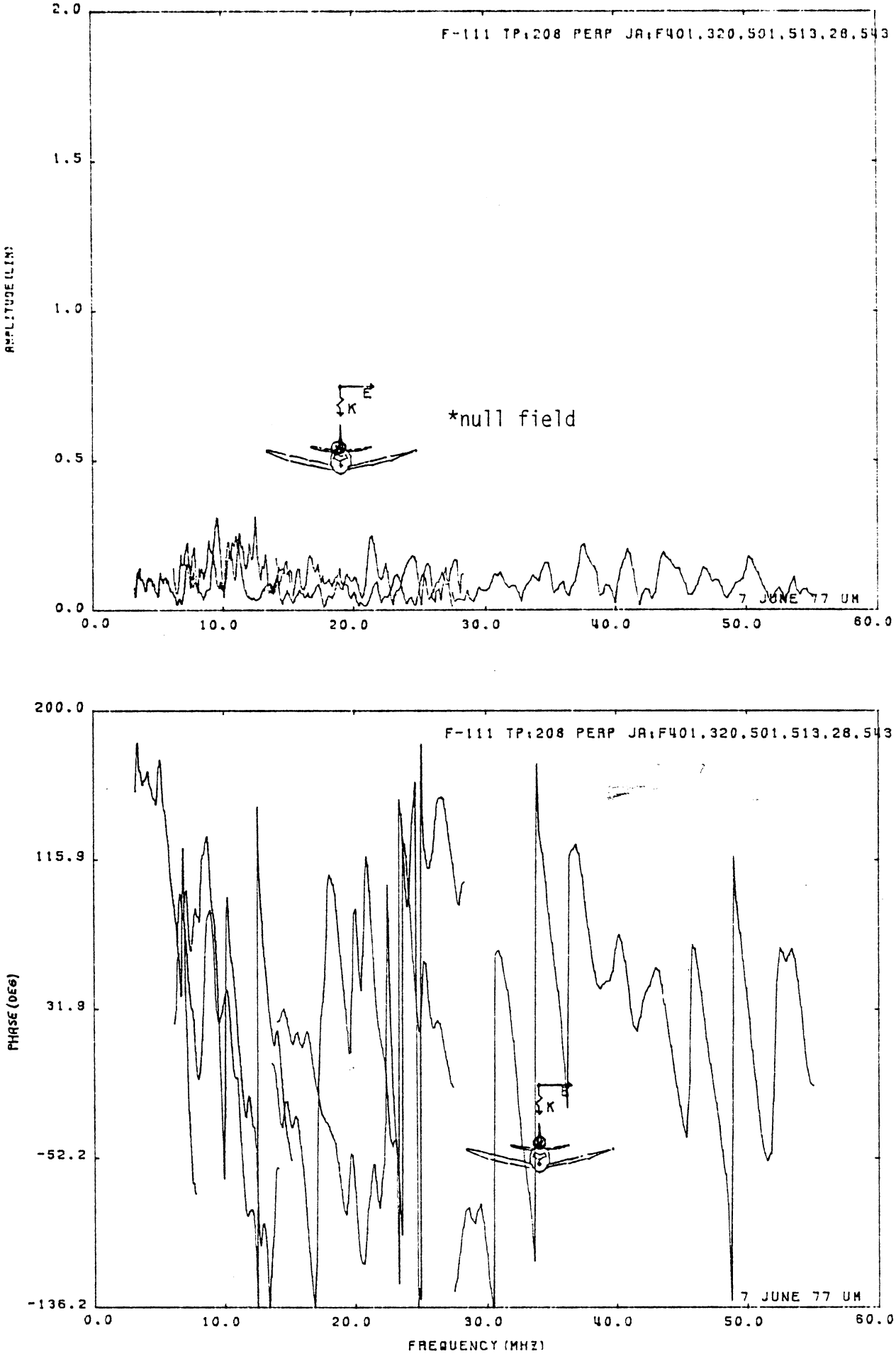

Figure 13: Axial current at TP:208, E-perpendicular to fuselage.

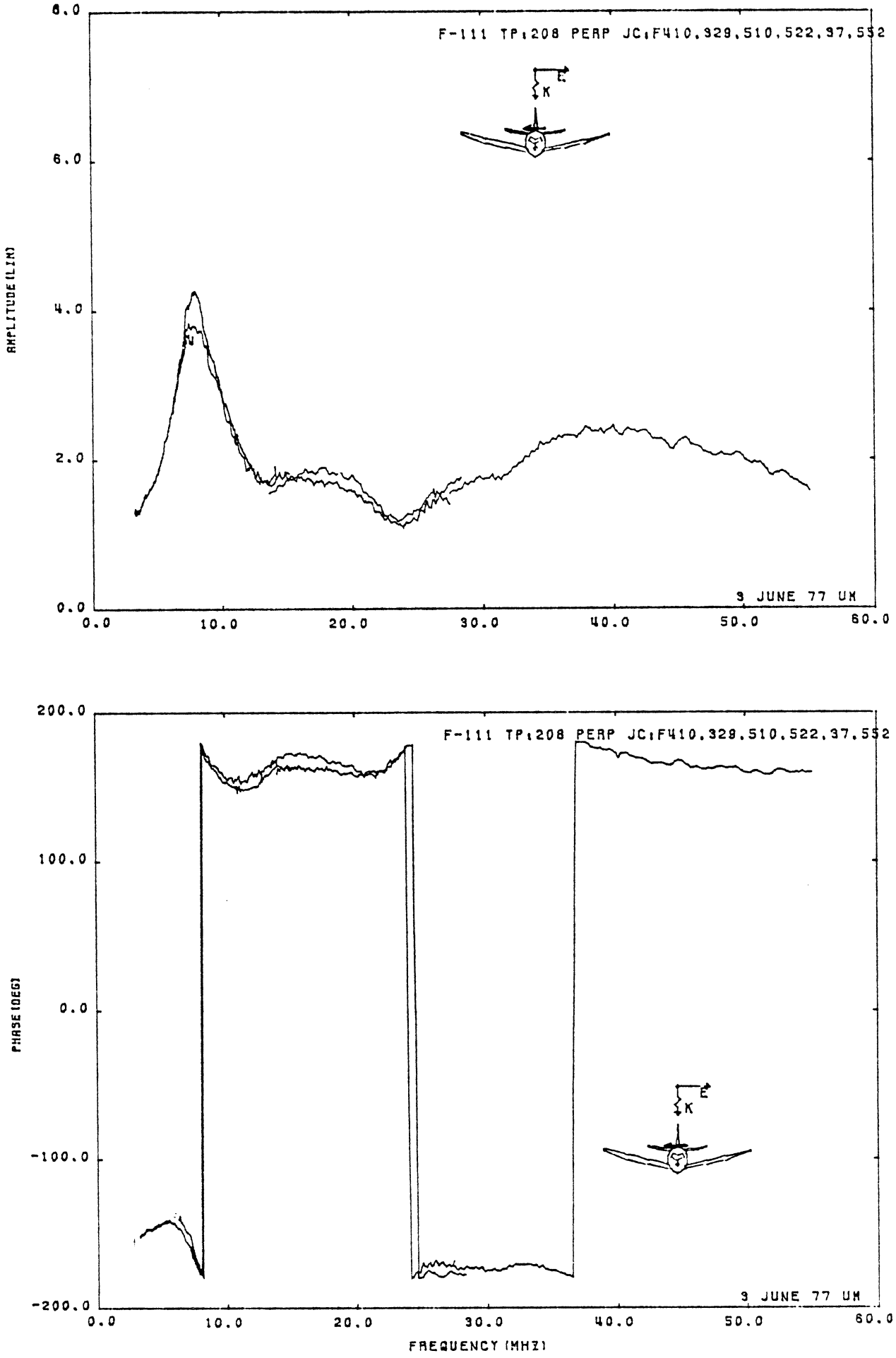

Figure 14: Circumferential current at TP:208, E-perpendicular to fuselage.

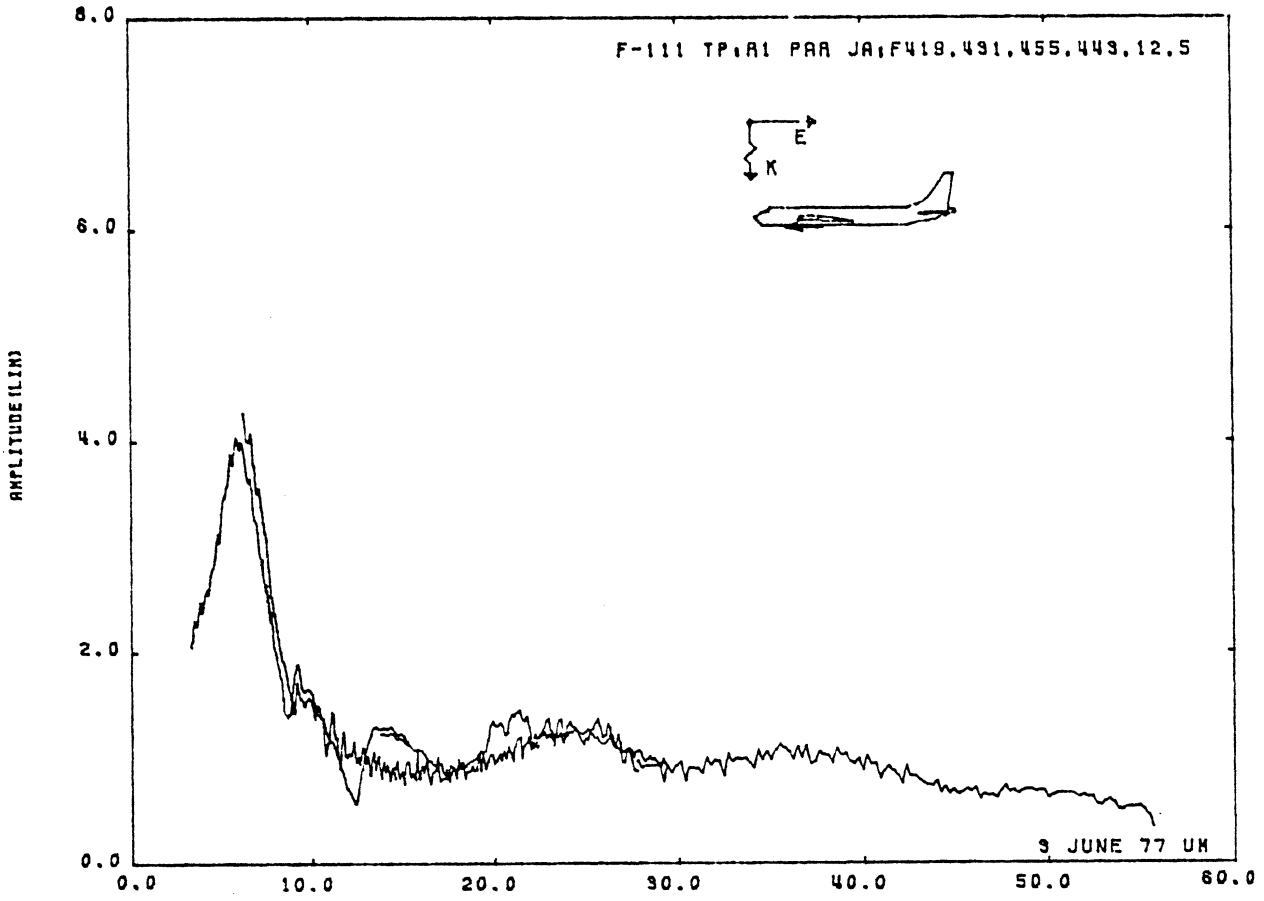

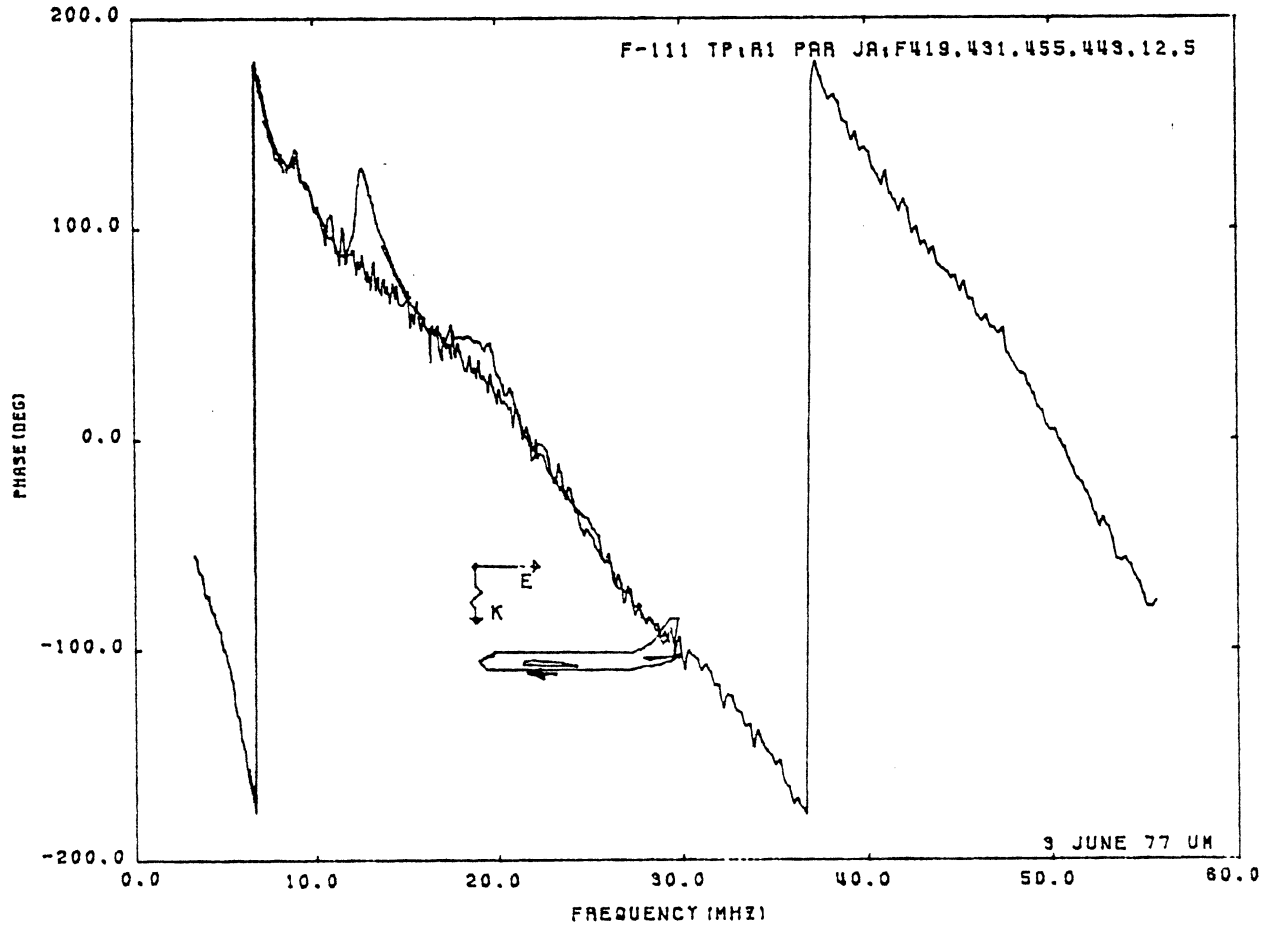

Figure 15: Axial current at TP:R1, E-parallel to fuselage.

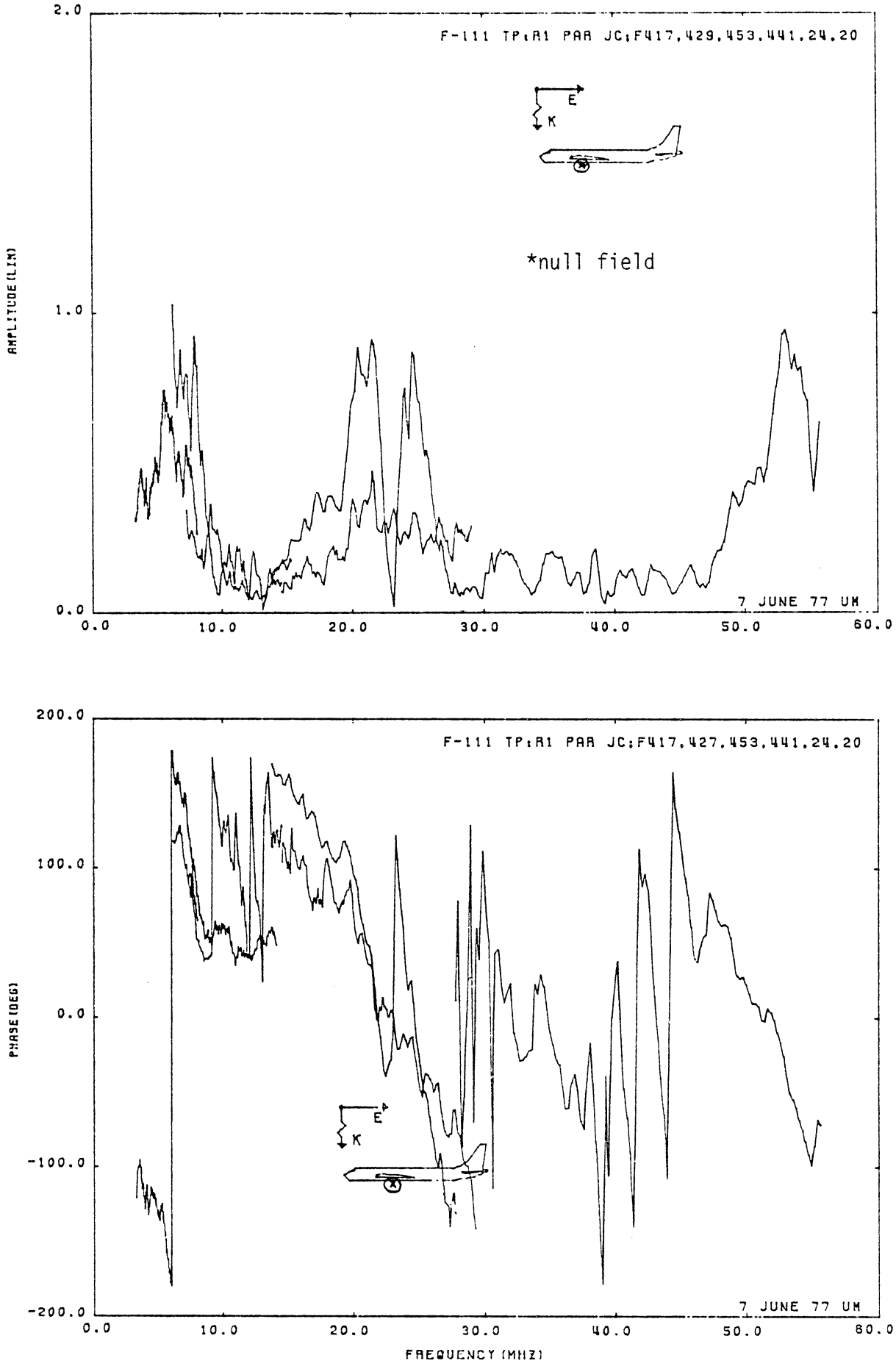

Figure 16: Circumferential current at TP:R1, E-parallel to fuselage.

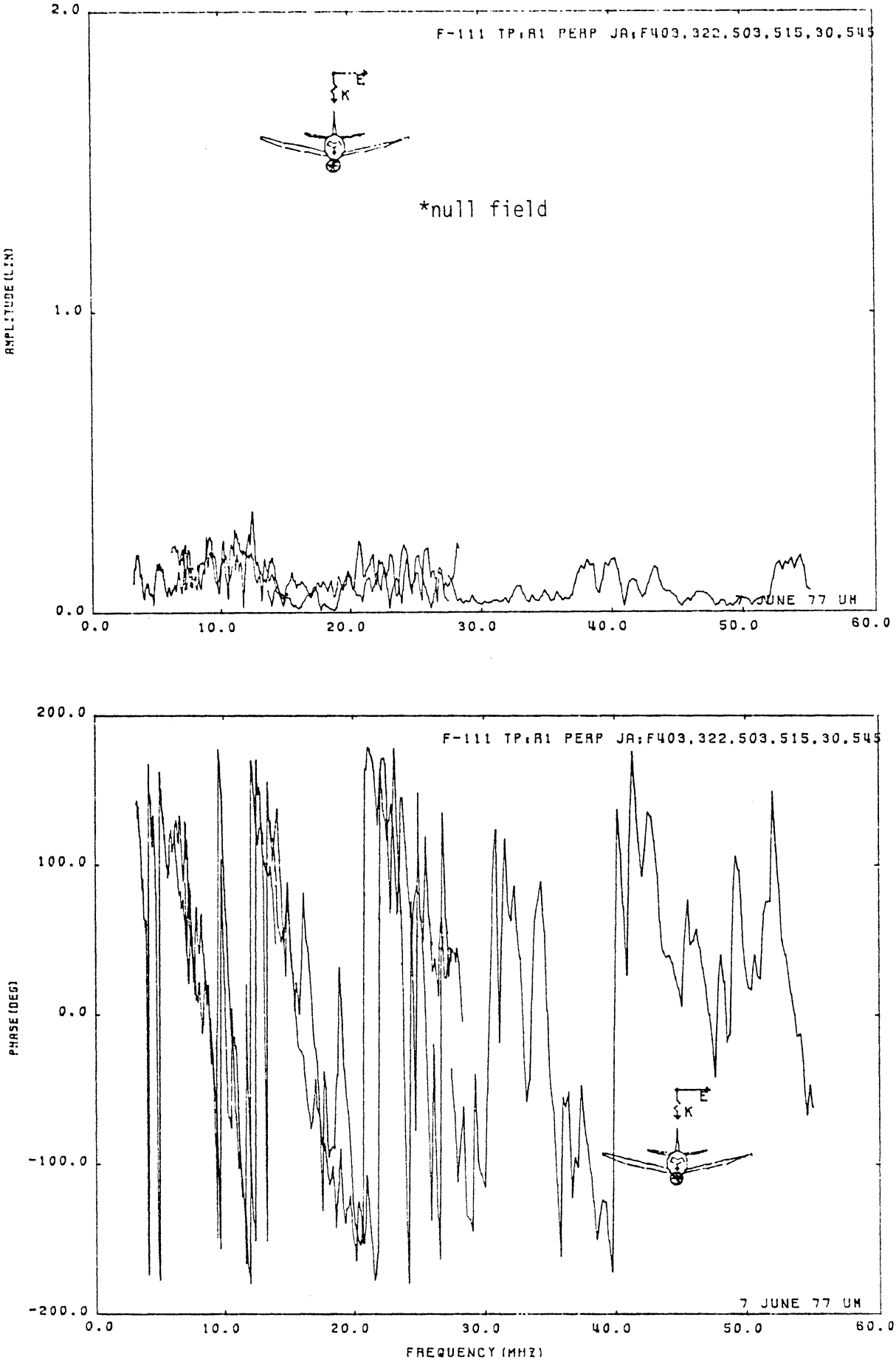

Figure 17: Axial current at TP:R1, E-perpendicular to fuselage.

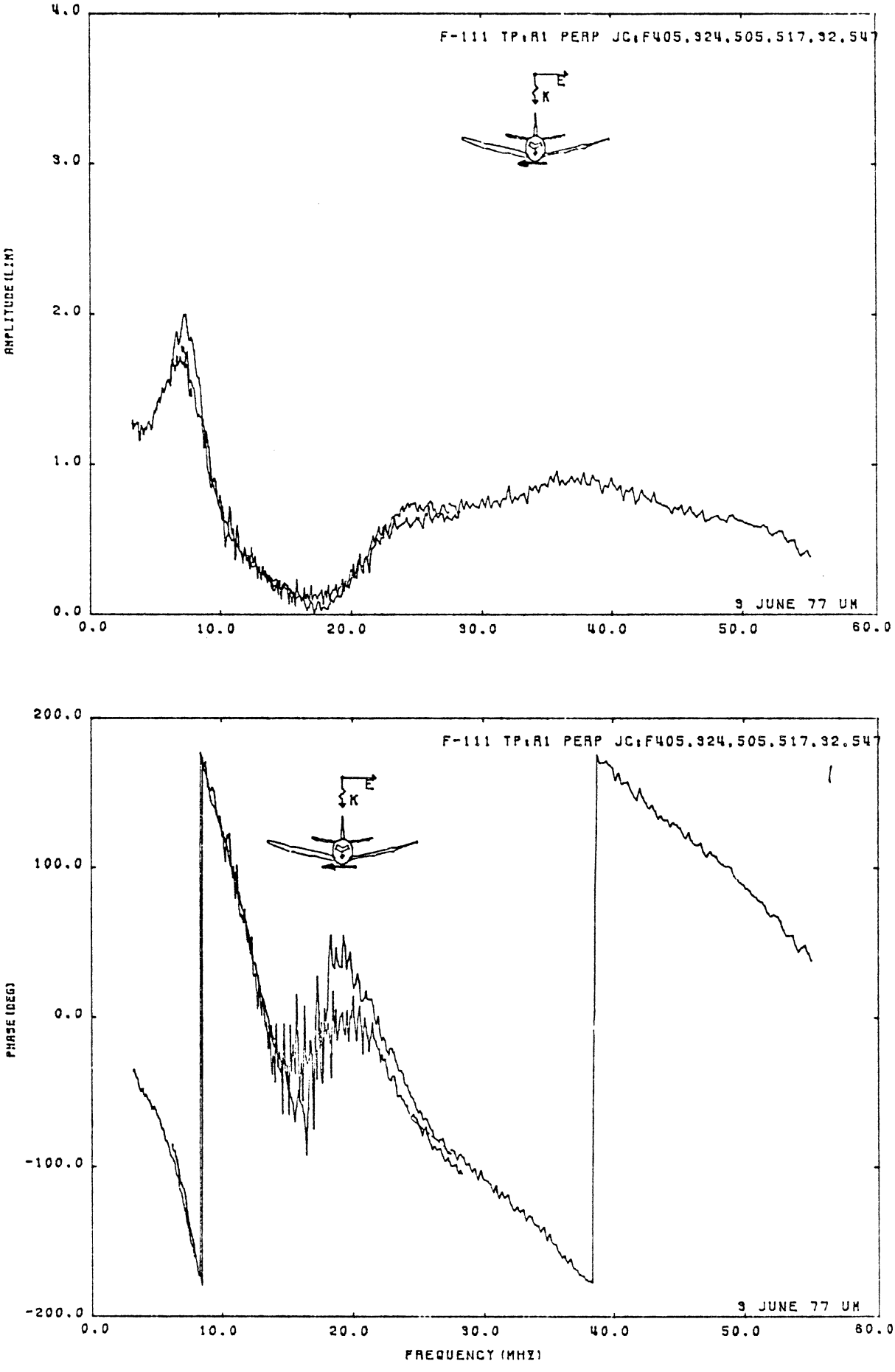

Figure 18: Circumferential current at TP:R1, E-perpendicular to fuselage.

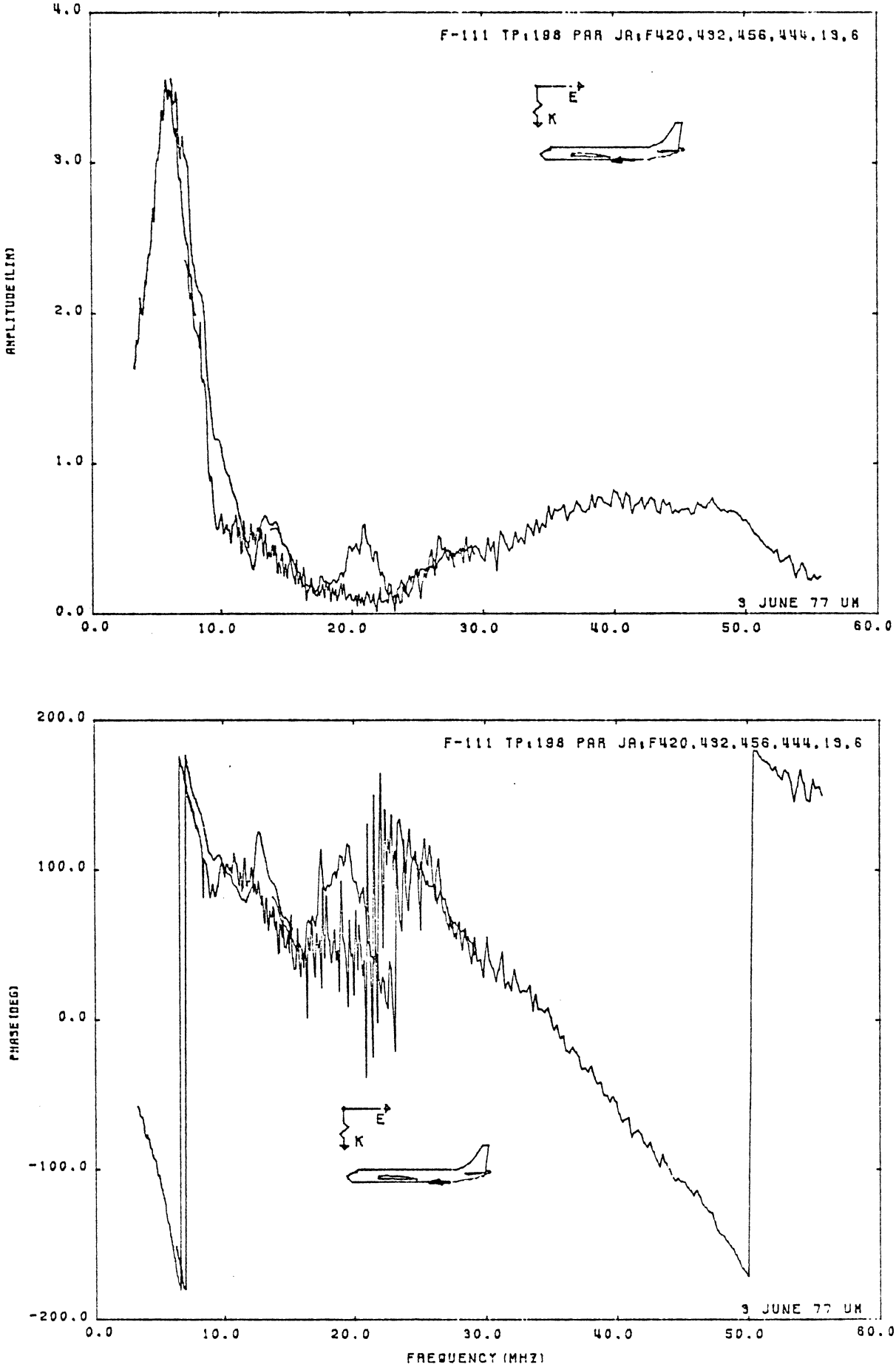

Figure 19: Axial current at TP:198, E-parallel to fuselage.

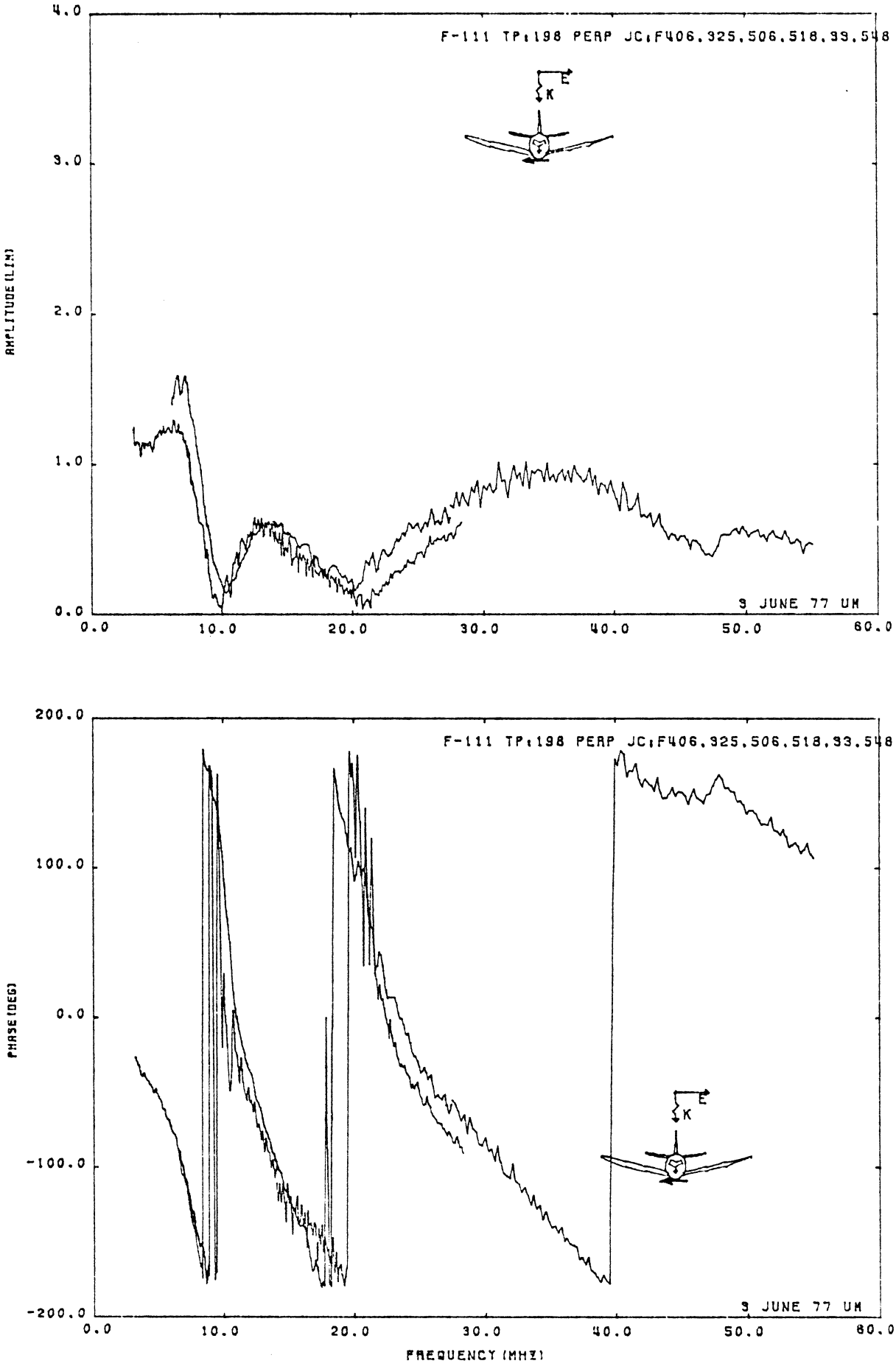

Figure 20: Circumferential current at TP:198, E-perpendicular to fuselage.

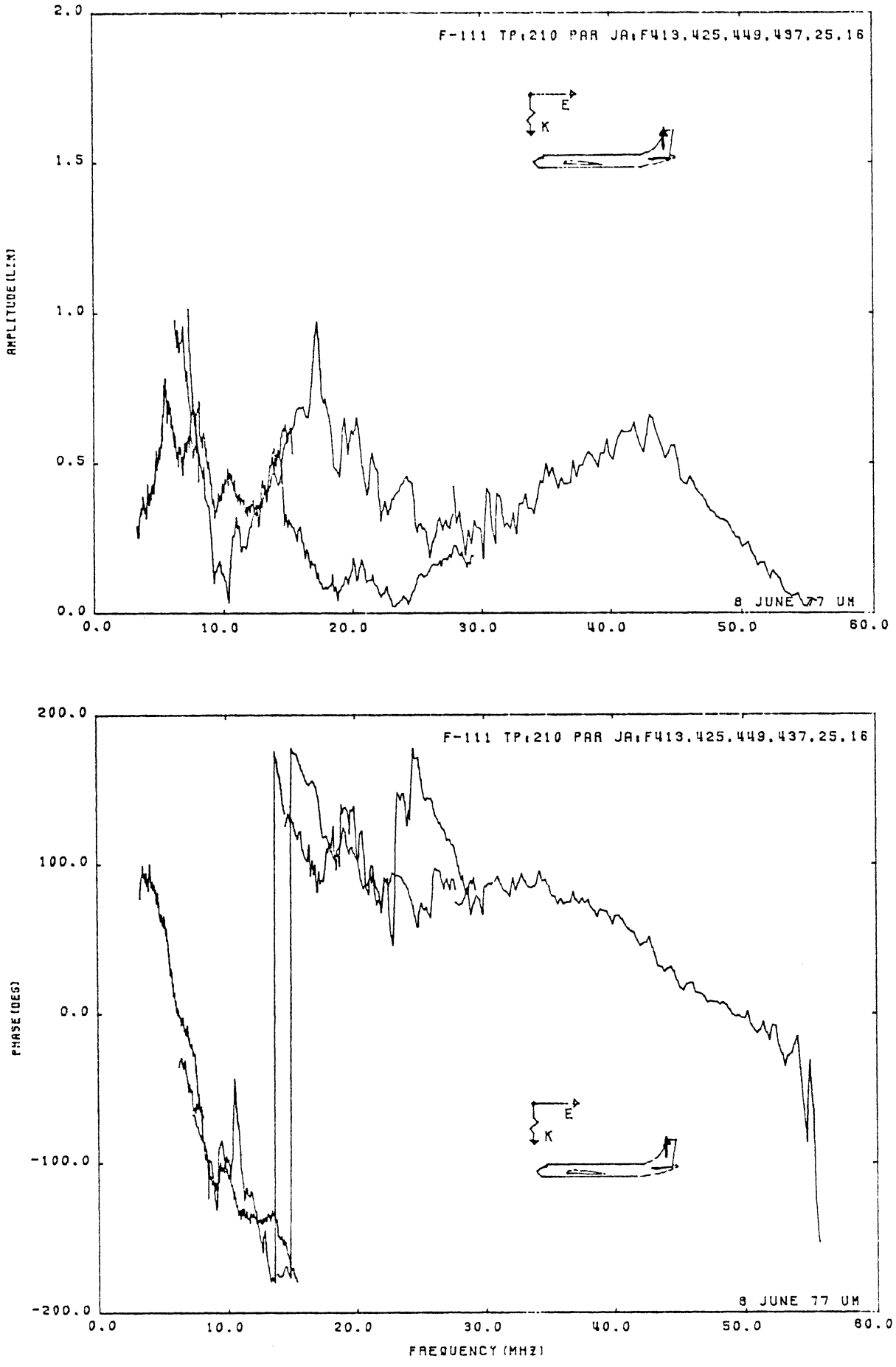

Figure 21: Axial current at TP:210, E-parallel to fuselage.

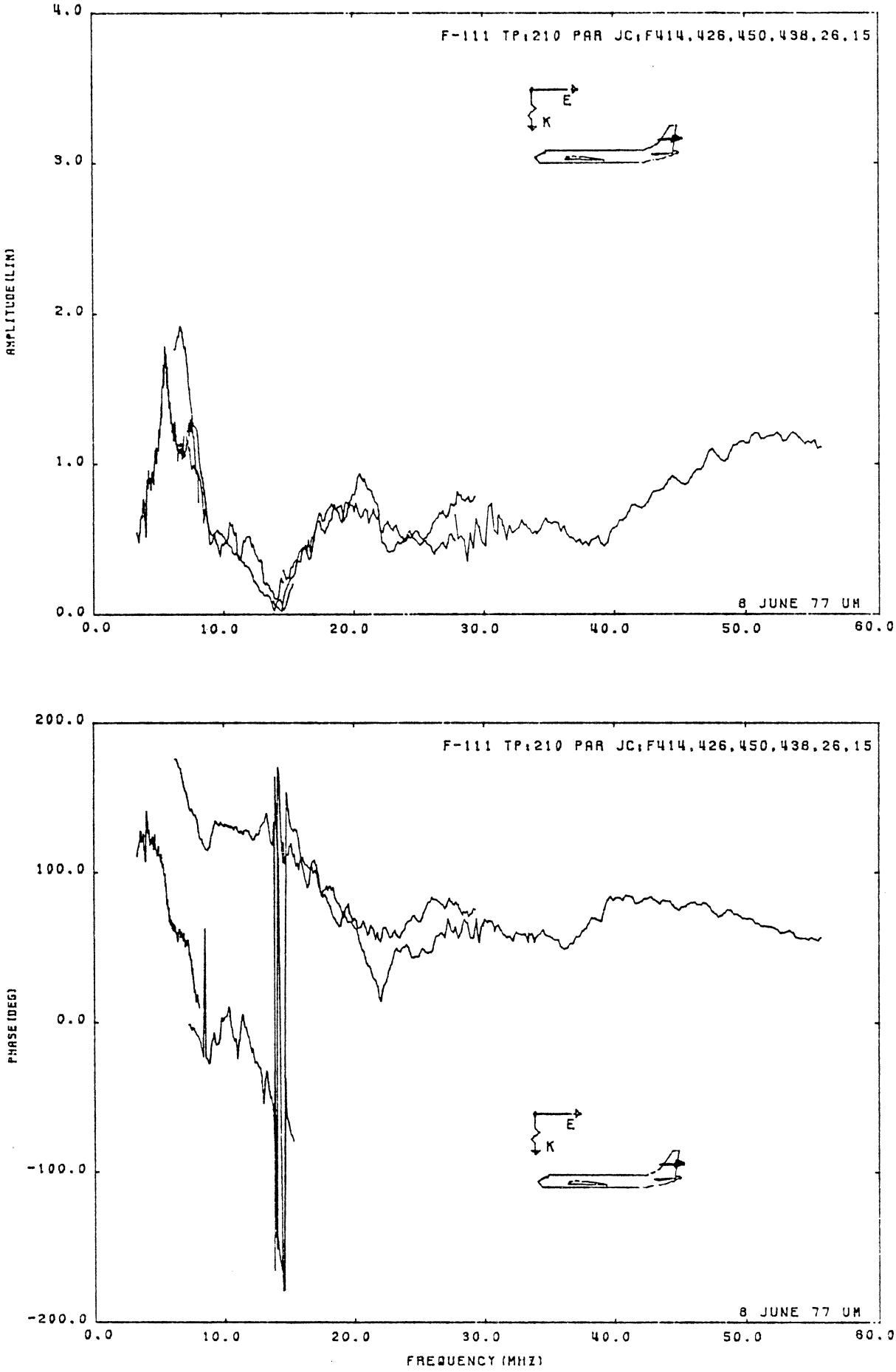

Figure 22: Circumferential current at TP:210, E-parallel to fuselage.

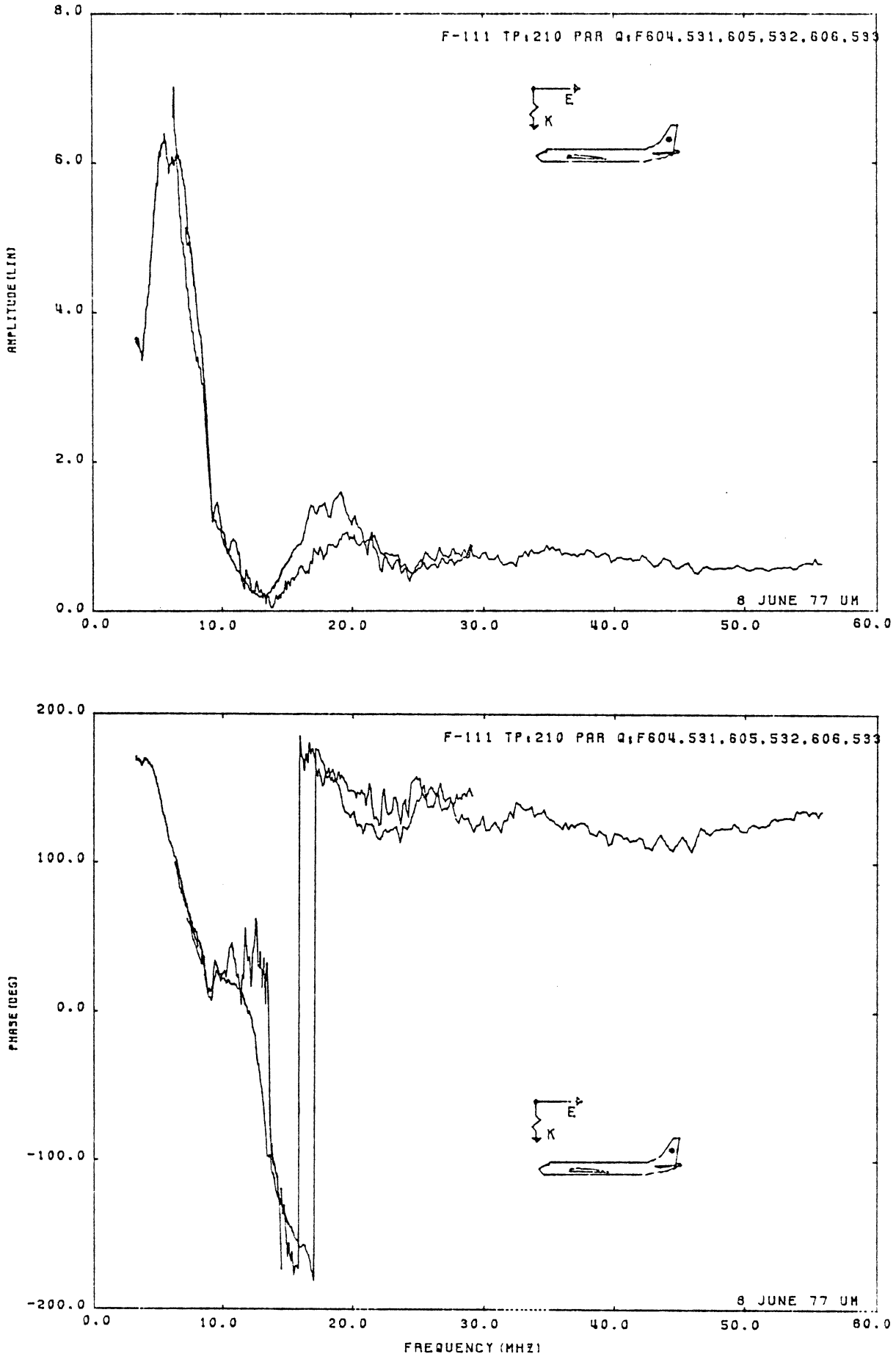

Figure 23: Charge at TP:210, E-parallel to fuselage.

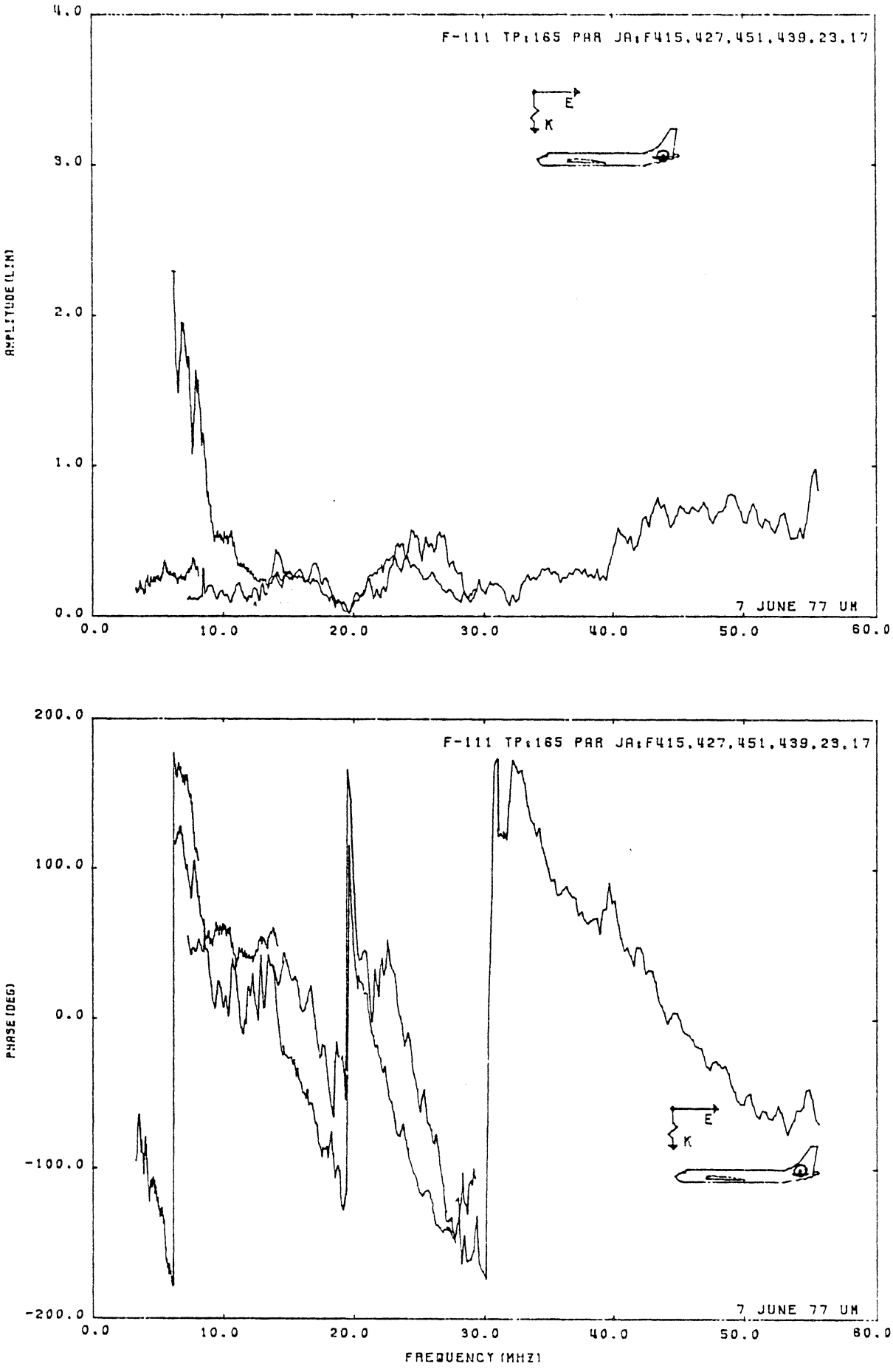

Figure 24: Axial current at TP:165, E-parallel to fuselage.

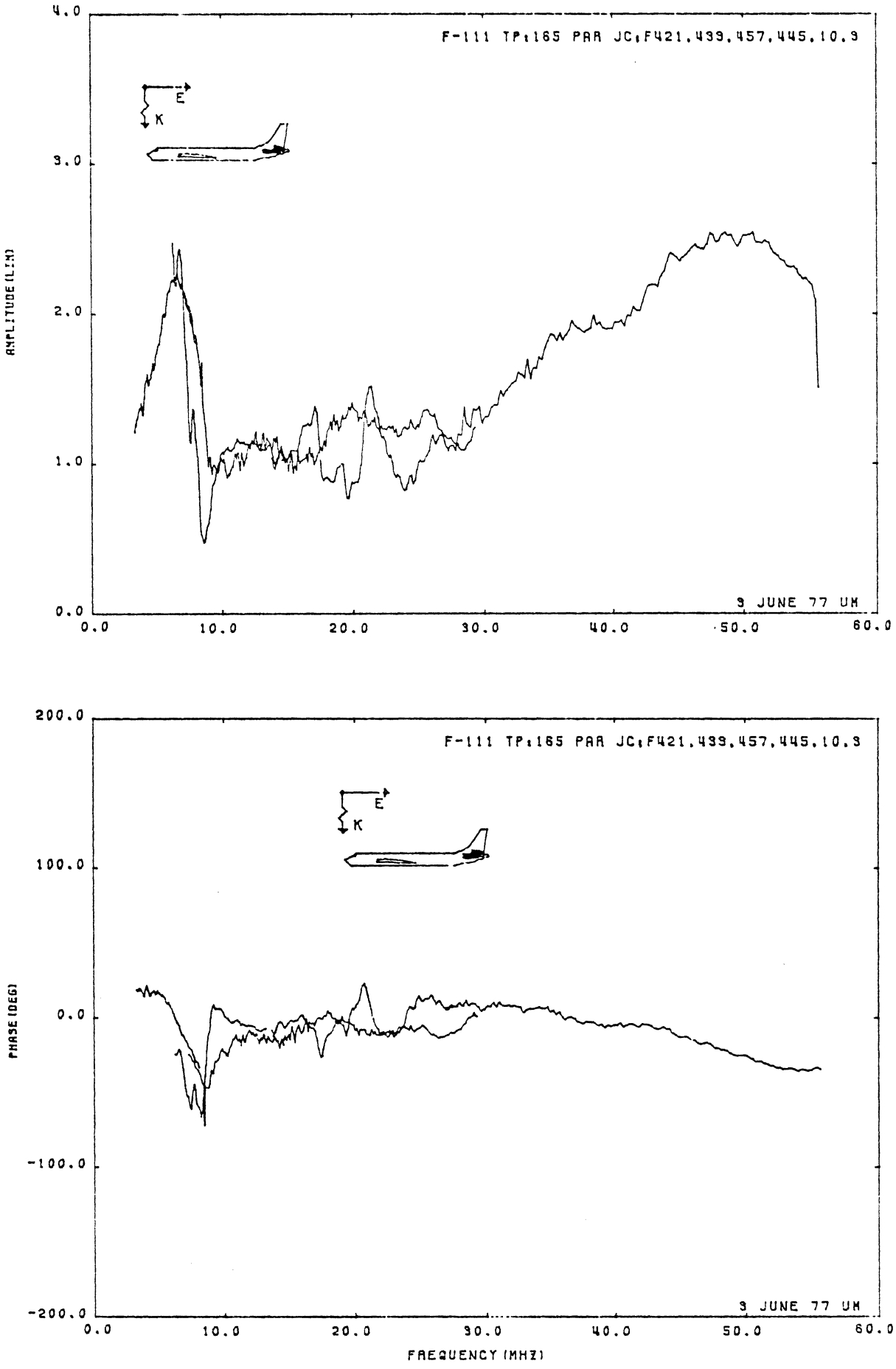

Figure 25: Circumferential current at TP:165, E-parallel to fuselage.

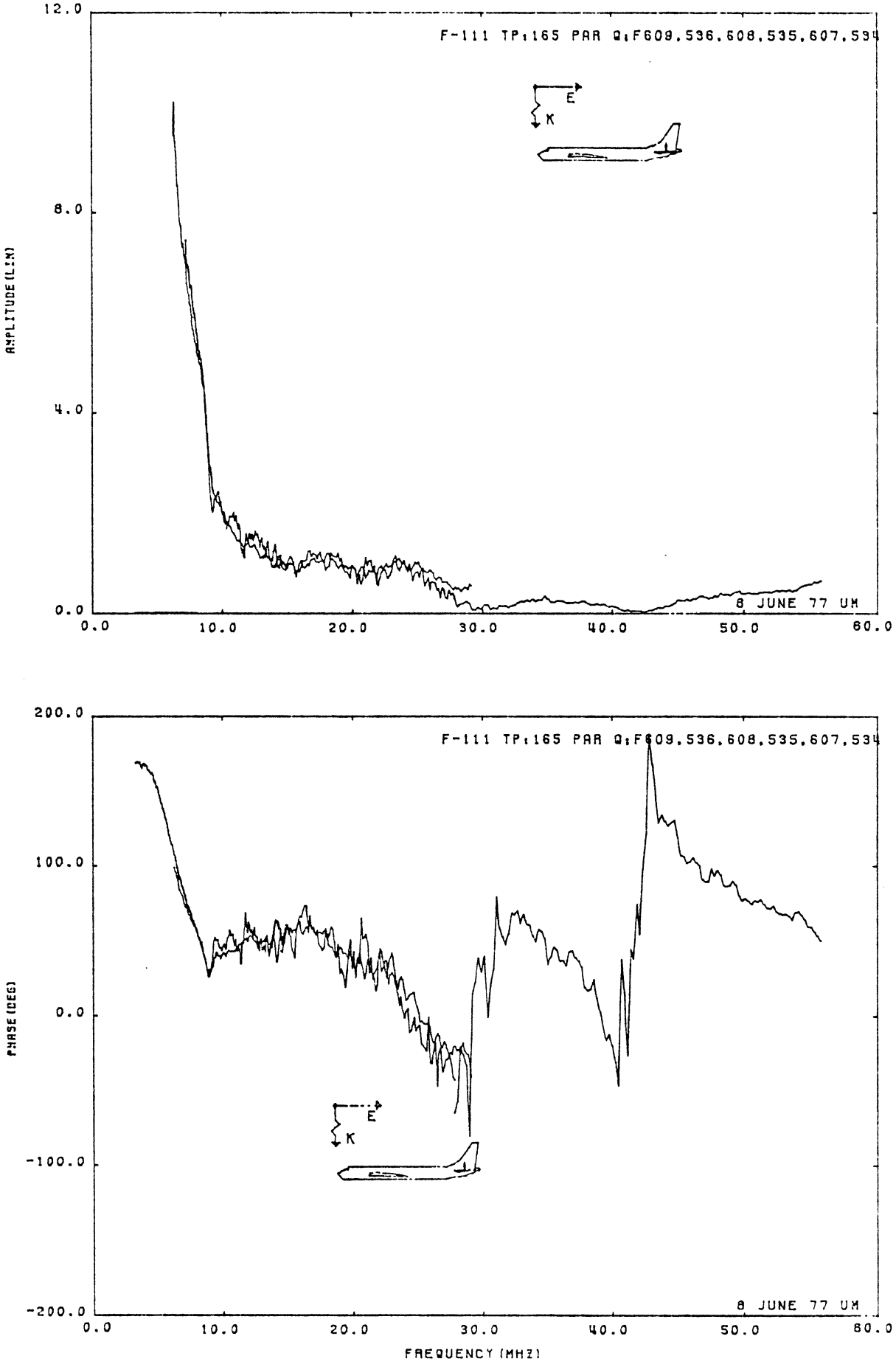

Figure 26: Charge at TP:165, E-parallel to fuselage.

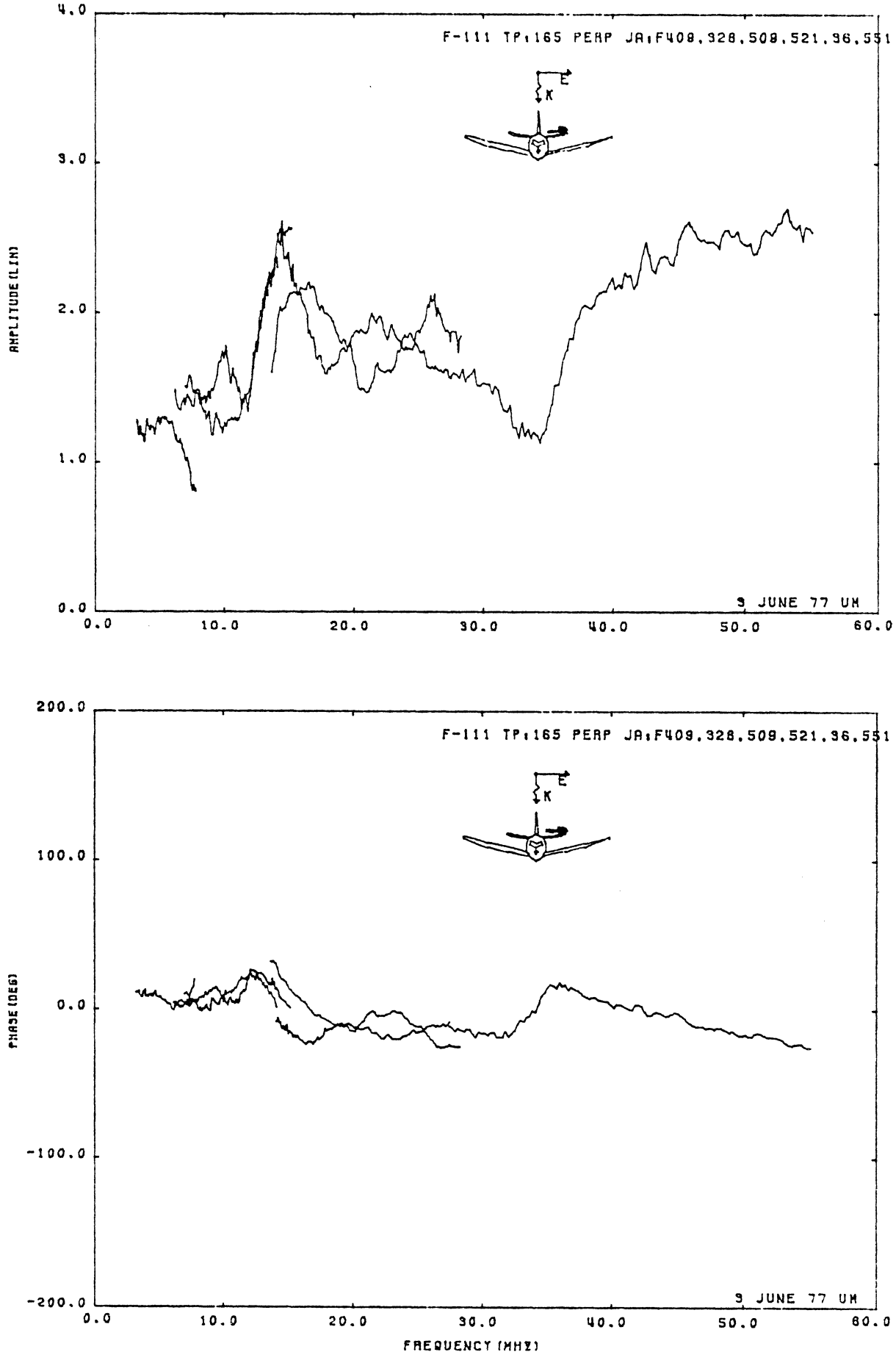

Figure 27: Axial current at TP:165, E-perpendicular to fuselage.

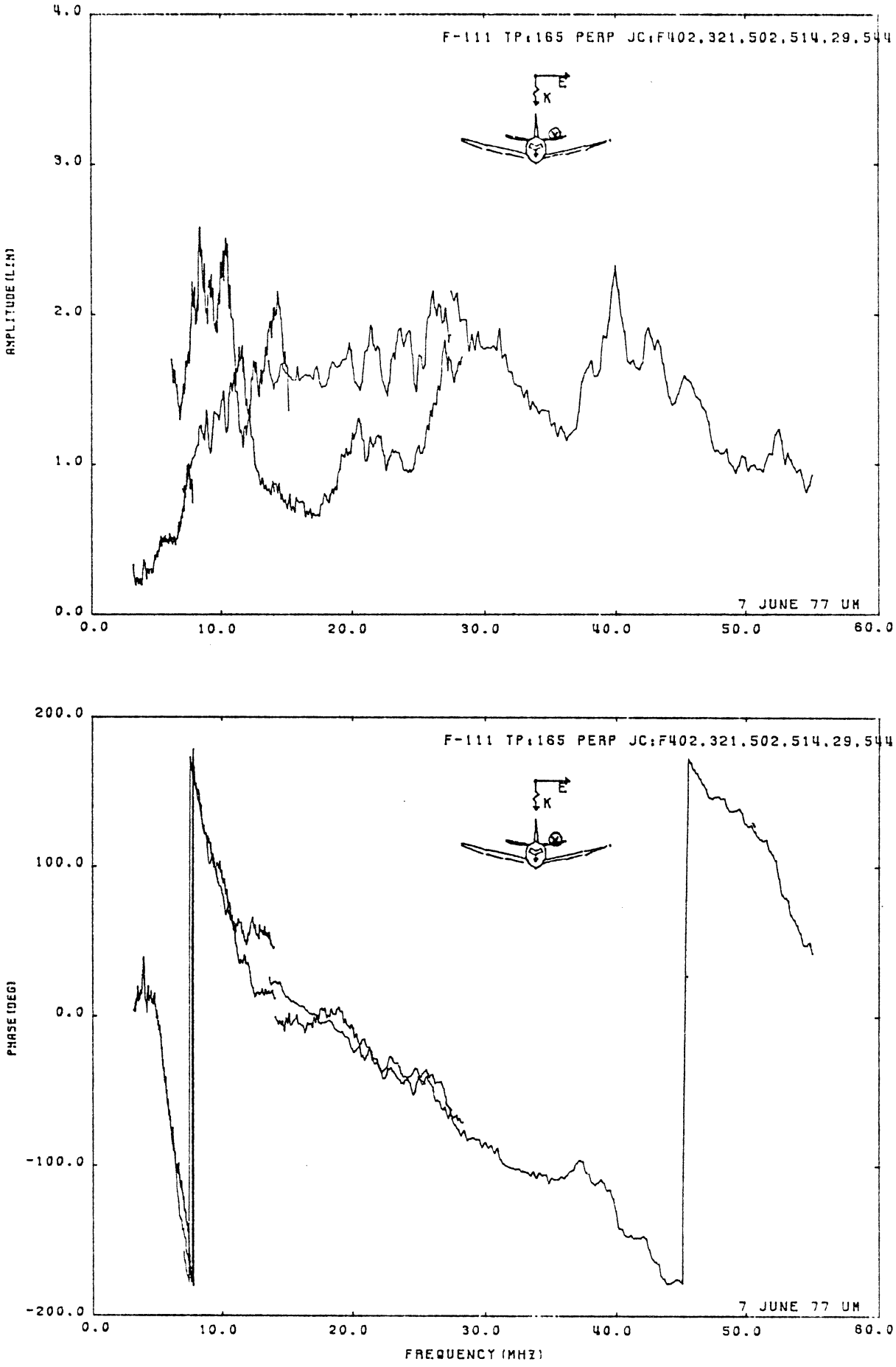

Figure 28: Circumferential current at TP:165, E-perpendicular to fuselage.

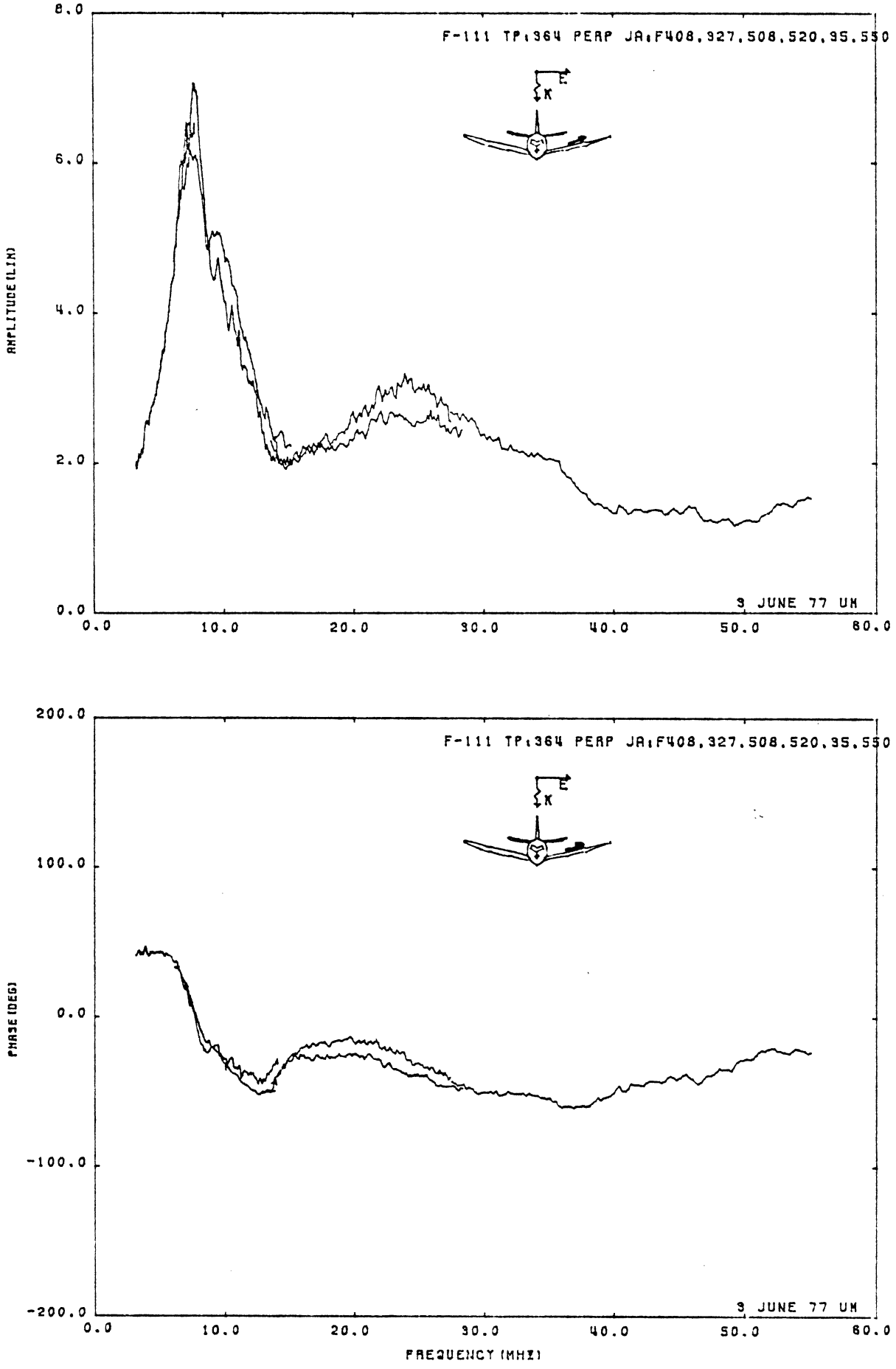

Figure 29: Axial current at TP:364, E-perpendicular to fuselage.

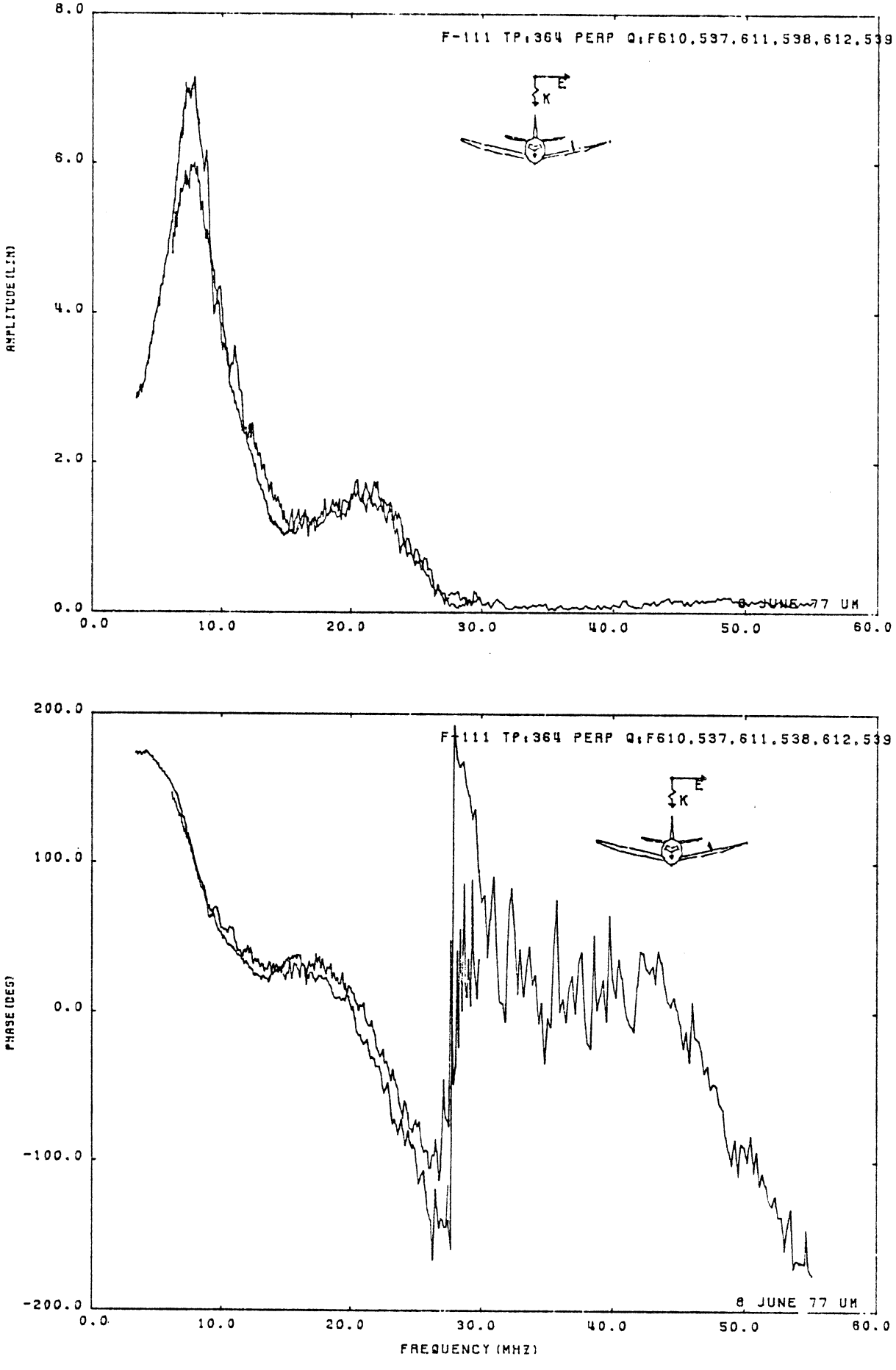

Figure 30: Charge at TP:364, E-perpendicular to fuselage.

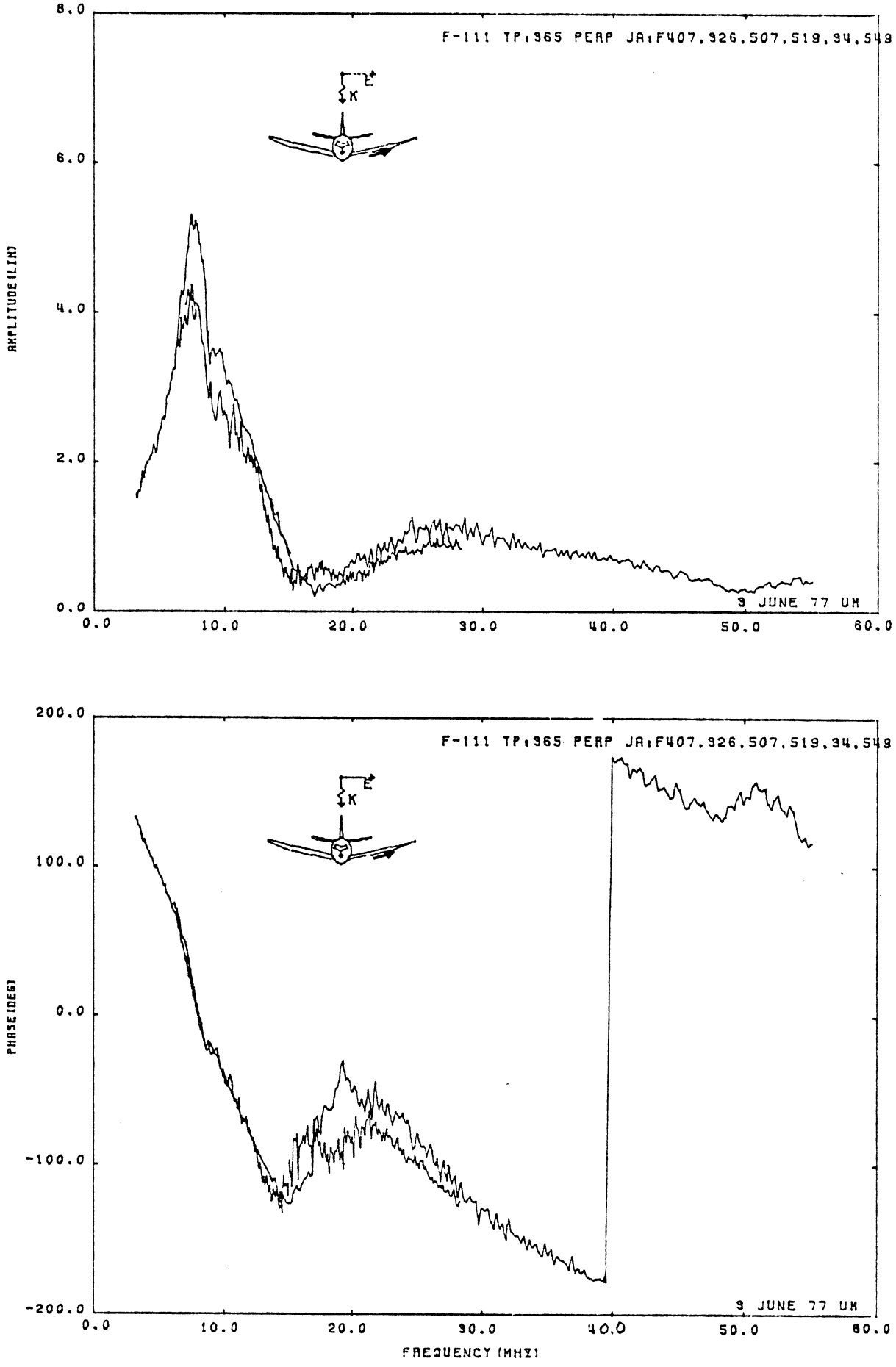

Figure 31: Axial current at TP:365, E-perpendicular to fuselage.

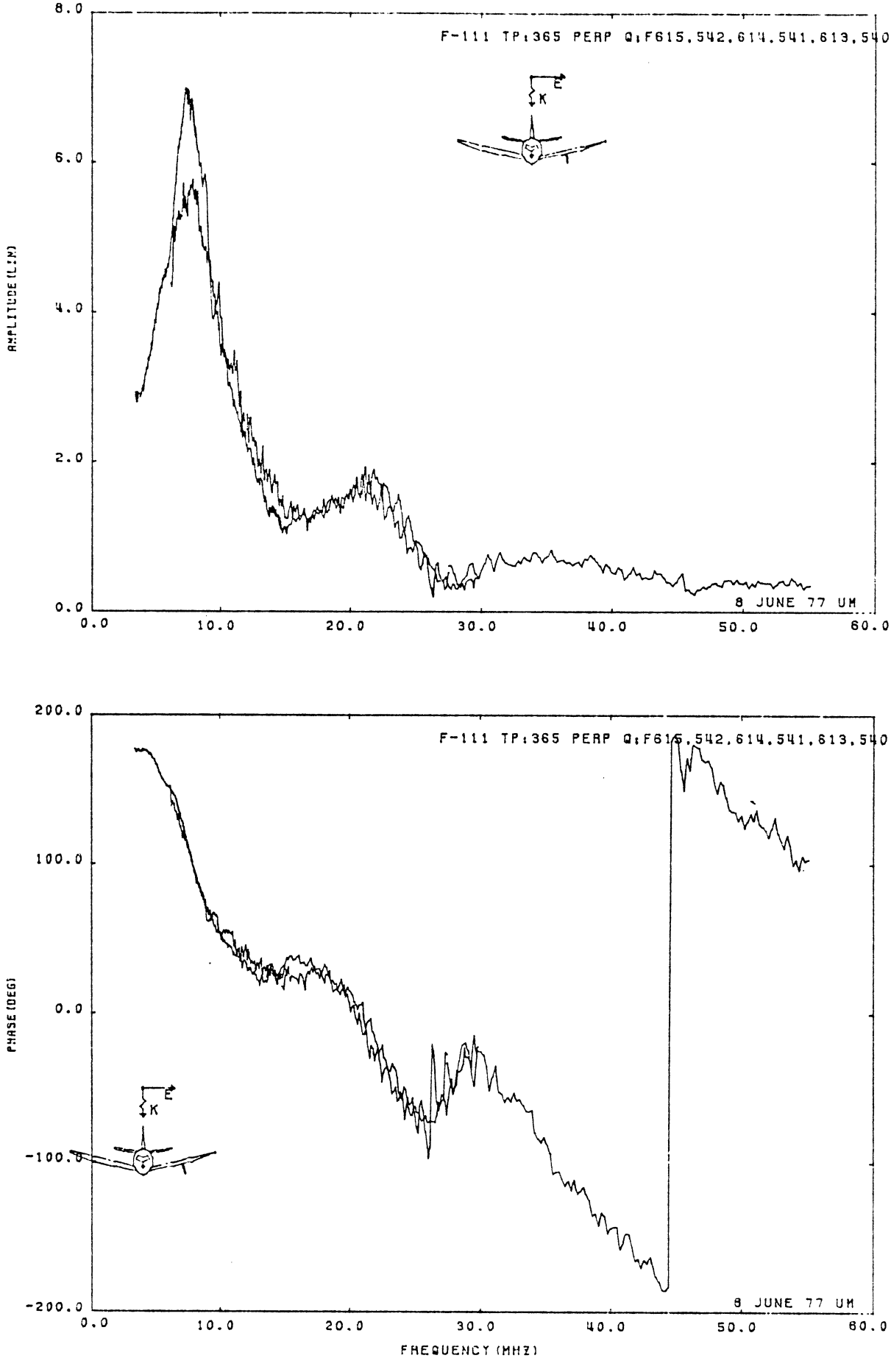

Figure 32: Charge at TP:365, E-perpendicular to fuselage.